Differences in Alimentary Glucose Absorption and Intestinal Disposal of Blood Glucose Following Roux-en-Y Gastric Bypass vs Sleeve Gastrectomy

Short title: Intestinal glucose handling after bariatric surgery

Jean-Baptiste Cavin[1], Anne Couvelard[1,2], Rachida Lebtahi[3], Robert Ducroc[1], Konstantinos Arapis[1,4], Eglantine Voitellier[1], Françoise Cluzeaud[1], Laura Gillard[1], Muriel Hourseau[2], Nidaa Mikail[3], Lara Ribeiro-Parenti[4], Nathalie Kapel[5], Jean-Pierre Marmuse[4,6], André Bado[1,6], Maude Le Gall[1]

[1]INSERM U1149, DHU Unity, Paris Diderot University, 75018, France
[2]Department of Pathology, Bichat hospital, AP-HP, Paris, 75018, France
[3]Department of Nuclear Medicine, Bichat hospital, AP-HP, Paris 75018, France
[4]Department of general and digestive surgery, Bichat hospital, AP-HP, Paris 75018, France
[5]Functional Coprology Service, Pitié Salpétrière Hospital Group, AP-HP, Paris, 75013, France
[6]Co-senior author

This work was supported by French minister of higher education and research, INSERM and University Paris Diderot.

BPL, bilio-pancreatic limb; GIP, glucose-dependent insulinotropic peptide; GLP1, glucagon-like peptide-1; GLUT, glucose transporter; RL, Roux limb; RYGB, Roux-en-Y gastric bypass; VSG, vertical sleeve gastrectomy; SGLT1, sodium/glucose cotransporter 1; PET/CT, positron emission and computed tomography.

Corresponding author:

Maude Le Gall Ph.D.

Gastrointestinal and Metabolic Dysfunctions in Nutritional Pathologies

Centre de Recherche sur l'Inflammation Paris Montmartre

Inserm UMRS 1149, Université Paris Diderot Paris 7,

Faculté de Médecine Site Bichat

16, rue Henri Huchard,

75890 Paris Cedex 18, France

Email:maude.le-gall@inserm.fr

Tel: +33 (0)157 277 459

Fax: +33 (0)157 277 471

The authors have declared that no conflict of interest exists

AUTHOR CONTRIBUTIONS

J.-B.C., M.L.G., A.B. and J.-P.M. designed the experiments; J.-B.C., M.L.G., A.B., F.C. and L.G. performed experiments; K.A. and E.V. performed animal surgeries; M.H., supervised by A.C., performed histologic analyses; N.M., supervised by R.L., performed PET/CT scan analyses; N.K. supervised stool analyses; R.D and J.-B.C. performed Ussing chamber analyses; J.-P.M., K.A. and L.R.-P. collected human clinical data and samples; J.-B.C., M.L.G., A.B., A.C., R.L. analysed and interpreted data; J.-P.M. supervised the human studies; J.-B.C., M.L.G. and A.B. wrote the manuscript with comments from A.C., R.D. and R.L.

KEY WORDS: intestinal adaptation; enteroendocrine cells; enterohormones; GIP

ABSTRACT

Background & Aims: Bariatric surgeries, such as Roux-en-Y gastric bypass (RYGB) or vertical sleeve gastrectomy (VSG), are the most effective approaches to resolve type 2 diabetes in obese individuals. Alimentary glucose absorption and intestinal disposal of blood glucose have not been directly compared between individuals or animals that underwent RYGB vs VSG. We evaluated in rats and humans how the gut epithelium adapts following surgery and the consequences on alimentary glucose absorption and intestinal disposal of blood glucose.

Methods: Obese male rats underwent RYGB, VSG, or sham (control) surgeries. We collected intestine segments from all rats; we performed histologic analyses and measured levels of mRNAs encoding the sugar transporters SGLT1, GLUT1, GLUT2, GLUT3, GLUT4 and GLUT5. Glucose transport and consumption were assayed using ex vivo jejunal loops. Histologic analyses were also performed on Roux limb sections from patients who underwent RYGB, 1–5 years after surgery. Roux limb glucose consumption was assayed following surgery by positron emission and computed tomography imaging.

Results: In rats and humans that underwent RYGB, the Roux limb became hyperplasic, with an increased number of incretin-producing cells, compared with the corresponding jejunal segment of controls. Furthermore, expression of sugar transporters and hypoxia-related genes increased and the non-intestinal glucose transporter GLUT1 appeared at the basolateral membrane of enterocytes. Ingested and circulating glucose was trapped within the intestinal epithelial cells of rats and humans that underwent RYGB. By contrast, there was no hyperplasia of the intestine after VSG, but the intestinal absorption of alimentary glucose was reduced and density of endocrine cells secreting glucagon-like peptide-1 (GLP1) increased.

Conclusions: The intestine adapts differently to RYGB vs VSG. RYGB increases intestinal glucose disposal, whereas VSG delays glucose absorption; both contribute to observed improvements in glycemia.

INTRODUCTION

The resolution of type 2 diabetes by bariatric surgery has attracted considerable attention in recent years. Diabetes resolves rapidly after Roux-en-Y Gastric Bypass (RYGB) or Vertical Sleeve Gastrectomy (VSG) [1]. Beyond postoperative weight loss, the surgical procedures themselves contribute to the cure of type 2 diabetes [2–5]. The described mechanisms so far involve caloric restriction [6–8], hormonal changes [9 10], accelerated gastric emptying [11–13] and bile acid signalling [9] but we still lack a clear understanding of the underpinning mechanisms. The gastrointestinal tract is the direct target of bariatric surgeries, and the early intestinal remodeling and adaptation triggered by such interventions could be the starting point for metabolic improvement [13]. Unquestionably, the small intestine contributes to glycemic control by orchestrating glucose transfer to the portal circulation after breakdown of complex carbohydrates to glucose. In addition, the gastrointestinal tract is an important endocrine organ with enteroendocrine cells secreting gut hormones, *i.e*., Glucagon-Like Peptide 1 (GLP1) and glucose-dependent Insulinotropic Peptide (GIP), involved in glucose-induced insulin secretion [14]. Most hypotheses propose that after RYGB, accelerated deliveries of nutrients to the distal gut, as well as duodenal exclusion, contribute to alterations in circulating gut hormone concentrations and improvement in glucose homeostasis [15].

The remodeling of gastrointestinal tract after RYGB surgery has been extensively studied in rat models and hyperplasia of the alimentary Roux limb (RL) was described in most reports [16–21]. This hyperplasia was associated with a reprogramming of intestinal glucose metabolism toward an increased glucose consumption to support tissue growth in a rat model of RYGB [19,21]. These recent observations contrast with previous studies reporting either a reduction in glucose uptake from the intestinal lumen [22] or no changes in intestinal glucose uptake *ex vivo* [23]. In addition, results of the literature regarding the expression pattern of intestinal sugar transporters after surgery are heterogeneous [17,19,22,24]. Glucose handling by the intestine is actually compartmentalized in two functional circuits: during the meals, alimentary glucose is absorbed and transferred to the portal blood, whereas at the fasted state, some glucose is

taken up from the arterial blood and used for intestinal metabolism [25]. Previous studies focus only on parts of this complex process, thus it remains unclear how the remodeled intestine absorbs and consumes alimentary and blood glucose after RYGB. One recent publication reported no hyperplasia of the jejunum and no reprogramming of intestinal glucose metabolism after SVG [21], however no study truly investigates the consequences of VSG on intestinal glucose handling.

In this study, we directly compared and contrasted the impact of RYGB and VSG surgeries on glucose handling by the intestine, distinguishing alimentary glucose transport from blood glucose intestinal uptake. In diet-induced obese rat models, the two surgeries differently alter intestinal morphology, enteroendocrine cell differentiation and glucose handling by the intestine in ways favourable for the regulation of glucose homeostasis. Finally, we extended our most important results to humans demonstrating that RYGB induces hypertrophy of the alimentary Roux limb with an increased number of incretin-producing cells and an unusual overexpression of the glucose transporter GLUT1 associated with a hypermetabolic activity of the epithelial cells.

MATERIALS AND METHODS

See Supplemental Experimental Procedures for detailed descriptions.

Animal surgeries and post-surgery procedures

All animal use conformed to the European Community guidelines was approved by the local ethics committee (N°#2011-14/773-0030 Comité d'Ethique Paris-Nord) and the Ministry of Higher Education and Research (N° 02285.01). Diet-induced obese rats were operated from Roux-en-Y gastric bypass (RYGB), sleeve gastrectomy (VSG) or sham surgery (sham) as previously described [26].

Human jejunal samples

Eight patients treated by surgery from November 2013 to July 2015 were retrospectively selected from the files of the department of pathology, Bichat Hospital, France. Mean age was 46.8±12.7 years at the time of the surgery and BMI was 55±5.6 for obese control group (n = 3) and 35.9±4.8 for RYGB patients (n = 5). None of them were diabetic and they had no medication to control their glycemia (See table S1).

Positron emission tomography

Seven patients were retrospectively selected from the files of the department of nuclear medicine, Bichat Hospital, France. Three RYGB patients and four control patients (without gastro-intestinal diseases or cancer) had been evaluated with [18F]-FDG PET/CT. In the RYGB group, mean age was 55.7 ± 7.6; BMI was 29.6 ± 3.2, in the control group, mean age was 64.5 ± 14.4; BMI was 30.6 ± 4.2; none of them were diabetic and they had no medication to control their glycaemia. PET and CT were performed with a PET/CT hybrid system (Discovery 690; GE Healthcare). See table S2 and Supplemental Experimental Procedures for detailed description of patients, procedure and image analyses.

Statistical analyses

All values are expressed as mean ± SEM. One-way ANOVA with Bonferroni correction for multiple comparisons were used to compare more than 2 groups and non-parametric Mann-Whitney tests were used to compare 2 groups. $P < 0.05$ was considered to be significant.

RESULTS

RYGB quickly induces hypertrophy of the alimentary Roux limb

We studied early events following RYGB surgery either in a diet-induced obese rat model (Text S1 and Figure S2). As soon as 2 weeks after surgery, the alimentary Roux limb (RL) was hypertrophic and displayed a dramatic increase in its diameter compared with that of the biliopancreatic limb (BPL) or with the corresponding jejunal segment (Jej) of sham-operated rats (Figure 1A). The villus height and crypt depth of the RL were increased leading to a thicker mucosa, whereas no modification of the BPL was observed (Figure 1B). The increase in average mucosal area was maintained over 40 days (Figure S3A). Moreover, the crypt cells in the hyperplasic RL were highly proliferative, as evidenced by the dense Ki67 immunostaining of mucosa (Figure 1C) and the increase in the number of Ki67-positive cells (Figure 1D).

Remarkably, in humans, the RL was hypertrophic with obvious increase in mucosal area (Figure 1E), increase in crypt depth (241 ± 37 µm vs 163 ± 10 µm in control group), but no changes in villus height (674 ± 35 µm vs 705 ± 16 µm in control group). The number of Ki67-positive cells was also increased (51 ± 7 cells/crypt vs 38 ± 1 cells/crypt in control group) (Figure 1F).

Increased number of endocrine cells in the hypertrophic alimentary Roux limb

A direct consequence of RL overgrowth was a local increased in the number of glucagon-like peptide (GLP1) (Figure 2A and 2B) and glucose-dependent insulinotropic peptide (GIP) producing cells (Figure 2C). Accordingly, glucose-induced GLP1 secretion increased (Figure S4). However, there were no significant changes in the average density of those enteroendocrine cells (Figure 2B and 2C). The same observations were made in RL from RYGB humans where no variation was found in the average density of enteroendocrine cells (*i.e.*, Chromogranin A-positive cells) or GLP1 secreting cells (Figure 2D and 2E).

Early and unusual expression of the glucose transporter GLUT1 in the alimentary Roux limb

We investigated the expression of various sugar transporters in the hyperplasic RL (Figure 3A and 3B) and the non-hyperplasic BPL (Figure S5A and S5B) after RYGB surgery in rats. Expression of genes encoding the prevalent intestinal transporters, *i.e.*, sodium-dependent glucose co-transporter 1 (SGLT1), and facilitative glucose transporter GLUT2 were not significantly increased two weeks after surgery whereas expression of fructose transporter GLUT5 tended to decrease (Figure 3A). However, SGLT1 transport activity measured in Ussing chamber doubled in the RL at 14 days (ΔIsc = 5.3 ± 0.5 µA/cm² in sham *versus* ΔIsc = 16.6 ± 5.6 µA/cm² in RL of RYGB $P<0.05$). The *Glut1* glucose transporter gene, normally barely expressed in mature intestine, was overexpressed in the hyperplasic RL (Figure 3A), but not in the BPL (Figure S4A). GLUT1 immunostaining on mucosa sections from the RL revealed strong basolateral GLUT1 expression both in rats and RYGB-patients (Figure 3C and 3D), showing a similar adaptive response to surgery in human. Interestingly, 40 days after surgery, *Glut1* mRNA levels remained high, but expression of genes encoding SGLT1, GLUT2 and GLUT5 had also increased in the RL (Figure 3B), but not in the BPL (Figure S5B). On the contrary, *Glut3* mRNA remained at a basal level (Figure 3A, 3B, S5A and S5B) and *Glut4* mRNA was never detected in the intestine (not shown). The appearance of GLUT1 incited us to measure the expression levels of the hypoxia-inducible genes. *Hif1α* mRNA increased in the RL and decreased in the BPL 14 days post-surgery in rats (Figure 3A and S5A) whereas the vascular endothelial growth factor *Vegf* mRNA, specifically increased in the RL 40 days after surgery (Figure 3B and S5B).

Increase sequestration of glucose in the alimentary Roux limb

We next questioned the functional impact of the modified expression of sugar transporters in the alimentary RL on intestinal glucose handling. We thus performed *ex vivo* transport studies on RL segments of rats subjected to RYGB and jejunal segments of sham-operated

rats, with radiolabeled [^{14}C]-glucose (Figure 4). The time-dependent transport of glucose from the mucosal side to the serosal side (mimicking alimentary glucose absorption) was identical in RYGB and sham groups, and sensitive to phloretin (Figure 4A). However, greater amounts of [^{14}C]-glucose were found within the RL mucosa after 60min (2,5 fold, P<0.001 vs. sham; Figure 4B). The transport of glucose from the serosal side to the mucosal side (mimicking blood glucose transport) was not affected by RYGB surgery (Figure 4C), but again greater amounts of [^{14}C]-glucose were measured after 60min within the RL mucosa at levels five times higher than that within the sham-operated jejunal segments (P<0.001 vs. Sham; Figure 4D). *In vivo*, the glycaemic response observed after an oral load of glucose in RYGB-rats was improved as soon as 14 days after RYGB surgery with a similar kinetic of glucose appearance in blood but an accelerated return to normal glycemia, compared to Sham-operated rats or preoperative animals (Figure 4E).

We next questioned the physiological relevance of these findings to humans, by reviewing Positron Emission Tomography-Computed Tomography (PET/CT) scan data for individuals that had undergone RYGB surgery. All analysed RYGB patients exhibited abnormal [^{18}F]-fluorodeoxyglucose ([^{18}F]-FDG) uptake by the intestine Roux limb. One exhibited a strong hypermetabolic activity in the RL characterized by an intense [^{18}F]-FDG uptake on attenuation-corrected PET images (Figure 4F and movie S1). The two other RYGB patients had also abnormal [^{18}F]-FDG uptake by the intestine Roux limb although more limited than the first patient. In comparison, no abnormal uptake was found in the corresponding jejunum of 4 control patients (matched for the body mass index) (Figure 4F and movie S1).

VSG does not induce intestinal hypertrophy but increases number and density of GLP1-positive cells

We next studied the jejunal remodeling in rats subjected to VSG (Text S2 and Figure S6). Two weeks after surgery, the jejunum was not hypertrophic and its diameter did not change compared with the jejunum of sham-operated rats (Figure 5A). The villus height but not the

crypt depth was slightly increased (Figure 5B). The average mucosal area did not change neither after 14 days (Figure 5B) nor after 40 days (Figure S3B). Accordingly, the number of Ki67-positive cells remained similar to that of sham-operated rats (Figure 5C). However, the number and density of GLP1- but not GIP-secreting cells were increased in the jejunum of VSG-operated rat after 14 days (Figure 5D and 5E). Accordingly, plasma GLP1 levels increased 30min after an oral glucose load in VSG-operated compared to sham-operated rats (Figure S4).

VSG does not induce GLUT1 and reduces intestinal absorption of glucose

Contrary to what we observed for hyperplasic RL after RYGB, no change in the expression level of prevalent jejunal sugar transporter occurred after VSG and induction of GLUT1 was detected neither 14 days nor 40 days after the surgery (Figure 6A). Time-dependent glucose transport from the mucosal side to the serosal side (mimicking alimentary glucose absorption) decreased markedly after VSG (Figure 6B). Moreover, the serosal-to-mucosal transport of [^{14}C]-glucose (mimicking blood glucose uptake) was slightly enhanced (Figure 6D). By contrast to RYGB where higher amounts of [^{14}C]-glucose were measured within the RL mucosa after 60min, the amounts of [^{14}C]-glucose was not significantly different in the jejunum mucosa of VSG-operated rats (whatever its alimentary or blood origin) (Figure 6C and 6E). *In vivo*, the glycaemic response observed after an oral load of glucose in VSG-operated rats improved, but with both a delayed appearance of glucose in blood (reduced absorption) and an accelerated return to normal, compared to sham-operated or preoperative animals (Figure 6F).

DISCUSSION

In this study, using diet-induced obese rats, we directly compared the impact of two bariatric surgeries on the glucose transport capacity of the intestine. We identified two distinct but rapid adaptations affecting intestinal morphology and glucose handling (Figure 7). In response to VSG, glucose transport capacity is reduced and density of cells secreting GLP1 is increased. In response to RYGB, the intestine became hyperplasic increasing *de facto* the number of GLP1-secreting cells but more importantly diverting glucose for its own growing needs. Both mechanisms are concomitant with an ameliorated glucose tolerance after surgery. Finally, the physiological relevance of these data was extended to obese individuals after RYGB.

It is usually accepted that enterohormones, in particular GLP1, play a role in glycaemic improvement after bariatric surgery [27]. In our rat studies, we confirmed that there were no significant changes in the average density of GLP1-producing enteroendocrine cells after RYGB surgery [21]. The same observations were made in RL from RYGB humans where no variation was observed in the average density of enteroendocrine cells (*i.e.*, Chromogranin A-positive cells) and GLP1 cells. Those results contrast with recent observations made by two different groups reporting an increased GLP1 and GIP cell density one year after RYGB in human [28,29]. However, a direct consequence of RL overgrowth after RYGB was a local increase in the number of GLP1- and GIP-producing cells. Thus, even in the absence of cell density modification, the enhanced intestinal mass directly leads to increase the secretory cell population, which in turn could contribute to enhance incretin secretion in response to stimulus as previously reported [18,30,31]. Interestingly, in our model of VSG-operated rat, the number and density of GLP1 cells was increased in the jejunum after 14 days. This observation contrasts with recent data showing that the number of GLP1-secreting cells did not change three months after VSG in rats [21]. Nevertheless it would be a reasonable explanation to the higher rate of GLP1 secretion that we observed with others [12]. Altogether our results suggest an early contribution of GLP1, in the amelioration of glycaemia following

surgery, but how the surgeries act on enteroendocrine cell distribution remains controversial. Kinetic analyses would allow determining whether the reported increase in GLP1 and GIP cell density is a transient phenomenon and could explain the discrepancy between early and later stage observations.

The hypertrophy of the RL after RYGB was previously reported in numerous rat models [16–21]. The similar average mucosal area observed 14 and 40 days after surgery in our RYGB rat model suggests that overgrowth of the RL is a very rapid process achieved within two weeks following surgery. The new morphometric characteristics of the RL are maintained over time, for at least one year after surgery in rodents [18,19]. This early RL response was characterised by the overexpression of a single sugar transporter, GLUT1, which is normally poorly expressed in mature jejunum [32]. GLUT1 has been shown to increase the supply of glucose to proliferative cancer cells in response to hypoxia [33]. Accordingly, levels of mRNA coding for the hypoxia-inducible factor HIF1 were found to have increased in the RL 14 days post-surgery in rats. This suggests that oxygen supply may be insufficient to support the massive hyperplasia. This hypothesis was strengthened by the additional overexpression of *Vegf* mRNA after 40 days. The HIF1 transcription factor directly regulates GLUT1 [34,35]. It could, therefore, initiate the reprogramming of glucose metabolism previously reported [19,21], providing the required additional energy. Concomitantly to the basolateral appearance of GLUT1, an enhancement of apical SGLT1 activity was measured in the RL of RYGB rats. Thus, apical SGLT1 may act together with basolateral GLUT1 to increase glucose uptake by the RL epithelium and allow energy requirements to be met. Intestinal transport studies revealed that greater amounts of absorbed glucose remained within the RL mucosa suggesting that the alimentary RL increases glucose uptake from the lumen during digestion, and consumes it to satisfy its own energy requirements. The increase in alimentary and circulating glucose uptake and consumption by RL epithelial cells may enhance glucose disposal during and between meals, thereby improving glycaemic control. A previous study, analysing [^{18}F]-FDG biodistribution in rats [19], ranked the remodelled intestine as the second

highest glucose consumer, after the brain. We next extend those results to humans. Gut hyperplasia following RYGB surgery, with appearance of glucose transporter GLUT1 at the basolateral membrane, leads to an increase in glucose consumption by the RL. The consequent glucose disposal, may contribute to the better glucose tolerance observed in rats and to the resolution of diabetes reported in humans [1]. One limitation of the present study is the small number of patients which renders delicate to draw strong conclusions about human intestinal adaptation. However, GLUT1 overexpression and hypermetabolic activity of the Roux limb observed in RYGB patients at different post-surgical stage provided evidence for the potential physiological relevance of these findings in humans.

Whereas the early induction of GLUT1 may be crucial to sustain the energy-consuming overgrowth of the intestine after RYGB, the subsequent overexpression of the other intestinal transporters, SGLT1, GLUT2 and GLUT5, could allow the increase in sugar absorption to counterbalance the malabsorption generated by the intestinal shortening. These two steps of intestinal adaptation processes may make different contributions to the early and long-term effects of RYGB surgery. They could reconcile previous controversial observations about expression patterns of sugar transporters after surgery [17,19,22,24].

Compared to RYGB, VSG is a less intrusive intervention involving surgical resection of a large part of the stomach, but results in a similar improvement in fasting glucose concentrations independently of weight loss [31,4]. Thanks to low complication rates and short hospital stays, VSG surgery is becoming the most popular bariatric surgery in developed countries. Nevertheless, little is known about its mechanisms of action and, to date, no study investigates the consequences of this surgery on intestinal glucose handling except one recent publication reporting no increase in hexokinase II protein expression after VSG versus RYGB [21]. Using our rat models, we directly compared and contrasted gut adaptation in response to VSG *versus* RYGB surgery. No hypertrophy of the jejunum mucosa, no induction of GLUT1 and no change in the expression level of prevalent jejunal sugar transporter occurred 14 days or 40 days after VSG. This absence of intestinal hypertrophy,

confirmed after three months in a recent study [21], shows that an increase in glucose disposal by the hypertrophic intestine is not likely to account neither for short-term nor for long-term improvements in glycaemia triggered by VSG. Consistently, no increase in the sequestration of glucose, whatever its origin (alimentary or blood), occurred in the jejunum of VSG-operated rats. However, the transport of alimentary glucose markedly decreased after VSG, suggesting that VSG jejunum had a lower absorption capacity of alimentary glucose. A slight but significant increase in transepithelial glucose transport from blood to the lumen was also detected. The origin of this regulation is unknown, but VSG may improve glucose tolerance by delaying the entry of alimentary glucose, and possibly by releasing some blood glucose into the lumen. These results were in agreement with the delayed glycaemic response observed after an oral load of glucose in our rats and reported in humans [36]. Intestinal remodelling could thus play a major role in the initial improvement of glucose homeostasis following both surgeries not only through better incretin secretion, but also through modified intestinal glucose handling. Another consequence of gastro-intestinal remodelling by bariatric surgery that we did not address in this study is accelerated gastric empting, although it may be important for incretin secretion and blood glucose delivery [11–13]. More interventional studies in rat models will be required to evaluate the relative contributions of each of these parameters to the regulation of glycemia.

Conclusion

In this study, we report that bariatric surgeries induce profound changes in glucose handling by the intestine although underlying mechanisms differ considerably between VSG and RYGB (Figure 7). In RYGB, alimentary glucose and blood glucose are sequestered by epithelial cells for their own use, whereas, in VSG, the uptake of alimentary glucose by the intestine is reduced. Further studies with more patients are needed to understand whether these adaptive mechanisms are key determinants for diabetes resolution in humans. Our results, nevertheless, unveil the reconfigured intestine as a putative contributor of glycemic

improvement and thwart the intuitive idea that RYGB and VSG must share a common mechanism of action for a similar efficiency.

REFERENCES

1. Rubino F, Schauer PR, Kaplan LM, et al. Metabolic Surgery to Treat Type 2 Diabetes: Clinical Outcomes and Mechanisms of Action. Annu. Rev. Med. 2010;61:393–411.

2. Pournaras DJ, Osborne A, Hawkins SC, et al. Remission of type 2 diabetes after gastric bypass and banding: mechanisms and 2 year outcomes. Ann. Surg. 2010;252:966–971.

3. Chambers AP, Jessen L, Ryan KK, et al. Weight-Independent Changes in Blood Glucose Homeostasis after Gastric Bypass or Vertical Sleeve Gastrectomy in Rats. Gastroenterology 2011;141:950–958.

4. Schauer PR, Bhatt DL, Kirwan JP, et al. Bariatric Surgery versus Intensive Medical Therapy for Diabetes — 3-Year Outcomes. N. Engl. J. Med. 2014;370:2002–2013.

5. Ardestani A, Rhoads D, Tavakkoli A. Insulin Cessation and Diabetes Remission After Bariatric Surgery in Adults With Insulin-Treated Type 2 Diabetes. Diabetes Care 2015;38:659–664.

6. **Isbell JM, Tamboli RA,** Hansen EN, et al. The Importance of Caloric Restriction in the Early Improvements in Insulin Sensitivity After Roux-en-Y Gastric Bypass Surgery. Diabetes Care 2010;33:1438–1442.

7. Lingvay I, Guth E, Islam A, et al. Rapid Improvement in Diabetes After Gastric Bypass Surgery. Diabetes Care 2013;36:2741–2747.

8. Lips MA, Groot GH de, Klinken JB van, et al. Calorie Restriction is a Major Determinant of the Short-Term Metabolic Effects of Gastric Bypass Surgery in Obese Type 2 Diabetic Patients. Clin. Endocrinol. (Oxf.) 2014;80:834–842.

9. Sweeney TE, Morton JM. Metabolic surgery: Action via hormonal milieu changes, changes in bile acids or gut microbiota? A summary of the literature. Best Pract. Res. Clin. Gastroenterol. 2014;28:727–740.

10. Holst JJ. Enteroendocrine secretion of gut hormones in diabetes, obesity and after bariatric surgery. Curr. Opin. Pharmacol. 2013;13:983–988.

11. Marathe CS, Rayner CK, Jones KL, et al. Relationships Between Gastric Emptying, Postprandial Glycemia, and Incretin Hormones. Diabetes Care 2013;36:1396–1405.

12. Chambers AP, Smith EP, Begg DP, et al. Regulation of gastric emptying rate and its role in nutrient-induced GLP-1 secretion in rats after vertical sleeve gastrectomy. Am. J. Physiol. - Endocrinol. Metab. 2014;306:E424–E432.

13. Seeley RJ, Chambers AP, Sandoval DA. The Role of Gut Adaptation in the Potent Effects of Multiple Bariatric Surgeries on Obesity and Diabetes. Cell Metab. 2015;21:369–378.

14. Campbell JE, Drucker DJ. Pharmacology, physiology, and mechanisms of incretin hormone action. Cell Metab. 2013;17:819–837.

15. Mingrone G, Castagneto-Gissey L. Mechanisms of early improvement/resolution of type 2 diabetes after bariatric surgery. Diabetes Metab. 2009;35:518–523.

16. Bueter M, Löwenstein C, Olbers T, et al. Gastric Bypass Increases Energy Expenditure in Rats. Gastroenterology 2010;138:1845–1853.e1.

17. Taqi E, Wallace LE, Heuvel E de, et al. The influence of nutrients, biliary-pancreatic secretions, and systemic trophic hormones on intestinal adaptation in a Roux-en-Y bypass model. J. Pediatr. Surg. 2010;45:987–995.

18. Mumphrey MB, Patterson LM, Zheng H, et al. Roux-en-Y gastric bypass surgery increases number but not density of CCK-, GLP-1-, 5-HT-, and neurotensin-expressing enteroendocrine cells in rats. Neurogastroenterol. Motil. 2013;25:e70–79.

19. **Saeidi N, Meoli L, Nestoridi E,** et al. Reprogramming of intestinal glucose metabolism and glycemic control in rats after gastric bypass. Science 2013;341:406–410.

20. Hansen CF, Bueter M, Theis N, et al. Hypertrophy Dependent Doubling of L-Cells in Roux-en-Y Gastric Bypass Operated Rats. PLoS ONE 2013;8:e65696.

21. Mumphrey MB, Hao Z, Townsend RL, et al. Sleeve Gastrectomy Does Not Cause Hypertrophy and Reprogramming of Intestinal Glucose Metabolism in Rats. Obes. Surg. 2015:1–6.

22. Stearns AT, Balakrishnan A, Tavakkolizadeh A. Impact of Roux-en-Y gastric bypass surgery on rat intestinal glucose transport. Am. J. Physiol. - Gastrointest. Liver Physiol. 2009;297:G950–G957.

23. Bhutta HY, Deelman TE, Roux CW le, et al. Intestinal sweet-sensing pathways and metabolic changes after Roux-en-Y gastric bypass surgery. Am. J. Physiol. - Gastrointest. Liver Physiol. 2014;307:G588–G593.

24. Nguyen NQ, Debreceni TL, Bambrick JE, et al. Upregulation of intestinal glucose transporters after Roux-en-Y gastric bypass to prevent carbohydrate malabsorption. Obesity 2014;22:2164–2171.

25. Fernández-López JA, Casado J, Argilés JM, et al. Intestinal handling of a glucose gavage by the rat. Mol. Cell. Biochem. 1992;113:43–53.

26. **Arapis K, Cavin JB,** Gillard L, et al. Remodeling of the Residual Gastric Mucosa after Roux-En-Y Gastric Bypass or Vertical Sleeve Gastrectomy in Diet-Induced Obese Rats. PLoS ONE 2015;10:e0121414.

27. Salehi M, D'Alessio DA. Effects of glucagon like peptide-1 to mediate glycemic effects of weight loss surgery. Rev. Endocr. Metab. Disord. 2014;15:171–179.

28. Rhee NA, Wahlgren CD, Pedersen J, et al. Effect of Roux-en-Y gastric bypass on the distribution and hormone expression of small-intestinal enteroendocrine cells in obese patients with type 2 diabetes. Diabetologia 2015:1–5.

29. **Nergård BJ, Lindqvist A,** Gislason HG, et al. Mucosal glucagon-like peptide-1 and glucose-dependent insulinotropic polypeptide cell numbers in the super-obese human foregut after gastric bypass. Surg. Obes. Relat. Dis. Off. J. Am. Soc. Bariatr. Surg. 2015.

30. Papamargaritis D, Miras AD, Roux CW le. Influence of diabetes surgery on gut hormones and incretins. Nutr. Hosp. 2013;28 Suppl 2:95–103.

31. Chambers AP, Jessen L, Ryan KK, et al. Weight-Independent Changes in Blood Glucose Homeostasis after Gastric Bypass or Vertical Sleeve Gastrectomy in Rats. Gastroenterology 2011;141:950–958.

32. Thorens B. Glucose transporters in the regulation of intestinal, renal, and liver glucose fluxes. Am. J. Physiol. - Gastrointest. Liver Physiol. 1996;270:G541–G553.

33. Szablewski L. Expression of glucose transporters in cancers. Biochim. Biophys. Acta BBA - Rev. Cancer 2013;1835:164–169.

34. Ebert BL, Firth JD, Ratcliffe PJ. Hypoxia and Mitochondrial Inhibitors Regulate Expression of Glucose Transporter-1 via Distinct Cis-acting Sequences. J. Biol. Chem. 1995;270:29083–29089.

35. **Chen C, Pore N,** Behrooz A, et al. Regulation of glut1 mRNA by Hypoxia-inducible Factor-1 interaction between H-ras and hypoxia. J. Biol. Chem. 2001;276:9519–9525.

36. Jiménez A, Ceriello A, Casamitjana R, et al. Remission of type 2 diabetes after Roux-en-Y gastric bypass or sleeve gastrectomy is associated with a distinct glycemic profile. Ann. Surg. 2015;261:316–322.

Author names in bold designate shared co-first author.

FIGURE LEGENDS

Figure 1. Hypertrophy and highly proliferative crypt cells in the Roux limb after RYGB surgery.

(A and C) Representative images of hematoxylin-phloxine-saffron (HPS)-stained section (A) or Ki67-immunostained section (C) of the alimentary Roux limb (RL) and biliopancreatic limb (BPL) of RYGB-rats and corresponding jejunal segment (Jej) from sham-operated rats 14 days post-surgery. Scale bar, 1 mm (A) and 100 µm (C).

(B and D) Morphometric analyses showing the mucosal area, villus height and crypt depth (B) and number of Ki67-immunoreactive cells per crypt (D) in the RL and BPL of RYGB-rats (n = 4), and jejunum from sham-operated rats (Jej) (n = 5) 14 days post-surgery. Data are means ± SEM. *P < 0.05, **P < 0.01 *versus* sham, based on ANOVA with Bonferroni correction for multiple comparisons.

(E and F) Representative images of HPS-stained (E) and Ki67-immunostained jejunum mucosa section (F) of RL mucosa from a patient who underwent RYGB (right), one year post-surgery, compared to a perioperative jejunum section from an obese individual (left). Scale bar, 500 µm.

Figure 2. Increased number of enteroendocrine cells after RYGB surgery.

(A) Representative images of GLP1 immunostaining in RL and BPL sections from RYGB-rats and jejunum from sham-operated rats 14 days post-surgery. Scale bar, 100 µm.

(B-C) Number of GLP1 (B) and GIP (C) immunoreactive cells per section and per mm² in the RL and BPL of rats after RYGB surgery (n = 4) or in the jejunum of sham-operated rats (n = 5), 14 days post-surgery. Data are means ± SEM. ***P < 0.001 *versus* sham, in ANOVA with Bonferroni correction for multiple comparisons.

(D-E) Representative images of Chromogranin A (D) and GLP1 (E) immunostaining in Roux limb sections from a patient who underwent RYGB (right), one year post-surgery and in the corresponding jejunum sections from an obese subject (left). Scale bar, 200 µm.

Figure 3. Early induction of the glucose transporter GLUT1 in the Roux limb after RYGB surgery.

(A and B) Relative mRNA levels for sugar transporters and hypoxia-inducible genes in the Roux limb mucosa at (A) 14 days (*n* = 4) or (B) 40 days (*n* = 5) after RYGB. The dotted lines indicate the mean mRNA levels of the corresponding genes in jejunal mucosa from sham-operated rats (*n* = 5). Data are means ± SEM. **P* < 0.05, ***P* < 0.01 *versus* sham-operated rats, in Mann-Whitney test.

(C) Representative images of GLUT1 immunostaining in Roux limb mucosa sections from RYGB-rats and corresponding jejunal sections from sham-operated rats 14 days post-surgery. Scale bar, 50 µm.

(D) Representative images of GLUT1 immunostaining in Roux limb sections from a patient who underwent RYGB, one year post-surgery and in the corresponding jejunum mucosa sections from an obese subject. Scale bar, 100 µm (upper panels). High magnification: lower panels. Scale bar 20 µm.

Figure 4. Increase in glucose consumption by the alimentary Roux limb after RYGB is associated with better oral glucose tolerance.

(A) Time course for the mucosal to serosal transport of [^{14}C]-glucose across the RL of RYGB-rats (*n* = 4) and the corresponding jejunum segment from sham-operated rats with (*n* = 3) and without (*n* = 8) phloretin, 14 days post-surgery.

(B) Mucosal [^{14}C]-glucose content of intestine segments at 60 minutes, showing greater sequestration of alimentary glucose within the RL from RYGB-rats (*n* = 4) than within the

equivalent jejunal segment from sham-operated rats (*n* = 8). Data are means ± SEM. ***P < 0.001, *versus* sham-operated rats, in Mann-Whitney tests.

(C) Time course for the serosal to mucosal transport of [^{14}C]-glucose across the RL of RYGB-rats (*n* = 4) and the corresponding jejunum segment from sham-operated rats with (*n* = 3) and without (*n* = 8) phloretin, 14 days post-surgery.

(D) Serosal [^{14}C]-glucose content of intestine segments at 60 minutes, showing greater sequestration of peripheral glucose within the RL from RYGB-rats (*n* = 4) than within the equivalent jejunal segment from sham-operated rats (*n* = 8). Data are means ± SEM. ***P < 0.001, *versus* sham-operated rats, in Mann-Whitney tests.

(E) Blood glucose levels after an oral load of glucose (1 g/kg) and the corresponding calculated area under the curve (AUC, inset) in obese rats before (preoperative, *n* = 12) and 12 days after RYGB (*n* = 4) or sham surgery (*n* = 5). Data are means ± SEM. *P < 0.05, **P < 0.01, *versus* the preoperative value, in two-way ANOVA followed by Bonferroni correction for multiple comparisons.

(F) Representative images from whole-body [^{18}F]-FDG PET/CT scan of a control individual and a RYGB patient. The blue arrowhead shows a strong [^{18}F]-FDG uptake by the Roux limb in patient who underwent RYGB (yellow-white signal) compared to the undetectable signal in the jejunum of BMI-matched control patient illustrating the hypermetabolic activity of the Roux limb in RYGB patient.

Figure 5. VSG does not induce intestinal hypertrophy but increases density and number of GLP1-positive cells. (A) Representative cross-sections of the jejunum of a VSG-rat and a sham-operated rat, 14 days post-surgery. Scale bar, 1 mm.

(B) Morphometric analyses of the jejunum showing the mucosal area of sections, villus height and crypt depth from VSG-rats (*n* = 5), compared with sham-operated rats (*n* = 5) 14 days post-surgery. Data are means ± SEM. *P < 0.05, NS (not significant), *versus* sham-operated rats, in Mann-Whitney test.

(C) Representative images of Ki67-immunostained sections and quantification of Ki67-positive proliferating cells in the crypts of jejunum from rats subjected to VSG or sham surgery, 14 days post-surgery. Scale bar, 100 µm. NS not significant, *versus* sham-operated rats, in Mann-Whitney test.

(D-E) Quantification of (D) GLP1 and (E) GIP-immunoreactive cells per section and per mm^2 of jejunum sections from VSG-rats (n = 4) and sham-operated rats (n = 5). Scale bar, 100 µm. Data are means ± SEM. *P < 0.05, NS not significant, *versus* sham-operated rats, in Mann-Whitney test.

Figure 6. VSG decreases intestinal glucose absorption. (A) Relative mRNA levels of sugar transporters in the jejunal mucosa from rats subjected to VSG 14 days (n = 4) or 40 days (n = 5) post-surgery. The dotted line indicates the mean mRNA levels in sham-operated rats (n = 5). Data are means ± SEM.

(B-D) Time course of mucosal-to-serosal (B) and serosal-to-mucosal (D) [^{14}C]-glucose transport across the jejunum of rats subjected to VSG (n = 6) and sham surgery, with (n = 3) or without (n = 8) phloretin, 14 days post-surgery. Data are means ± SEM. *P < 0.05, **P < 0.01, ***P < 0.001, *versus* sham-operated rats, in two-way ANOVA with Bonferroni correction for multiple comparisons.

(C-E) [^{14}C]-glucose content of intestine segments at 60 minutes. No significant difference in the sequestration of alimentary (C) or peripheral (E) glucose within the jejunal segments was observed between VSG and sham-operated rats. Data are means ± SEM. NS, not significant, in Mann-Whitney test.

(F) Blood glucose levels after administration of an oral load of glucose (1 g/kg) and the corresponding calculated area under the curve (AUC, insert) in obese rats before (preoperative, n = 16) and 12 days after VSG (n = 5) or sham surgery (n = 9). Data are means ± SEM. $^{\#}P$ < 0.05 (sham vs. preoperative), **P < 0.01, ***P < 0.001 (VSG vs. preoperative), in two-way ANOVA with Bonferroni correction for multiple comparisons.

Figure 7. Schematic view of the differential intestinal adaptations after RYGB and VSG leading to improvement of glucose tolerance

In response to RYGB, the intestine became hyperplasic, alimentary glucose transport and blood glucose uptake increased but glucose was sequestered by epithelial cells for their own use. In response to VSG, alimentary glucose transport capacity was reduced and a slight increase in transepithelial glucose transport from blood to the lumen was detected. Both intestinal adaptations contribute to ameliorate sugar tolerance after surgery.

ACKNOWLEDGMENT

We would like to thank the team of N.K. at Department of Functional coprology, APHP for stool analyses; Pr D. Le Guludec responsible of FRIM imaging platform and Chief of the Nuclear Physic Department; O. Thibaudeau and S. Ameur for help in histologic experiments; V. Descatoire for help in histologic analyses; L. Aline for technical help; J. Le Beyec, H. Duboc and S. Ledoux for comments. M.L.G. thanks L. Arnaud for constant support.

Figure 1

Click here to download Figure: Cavin et al Figure 1.tif

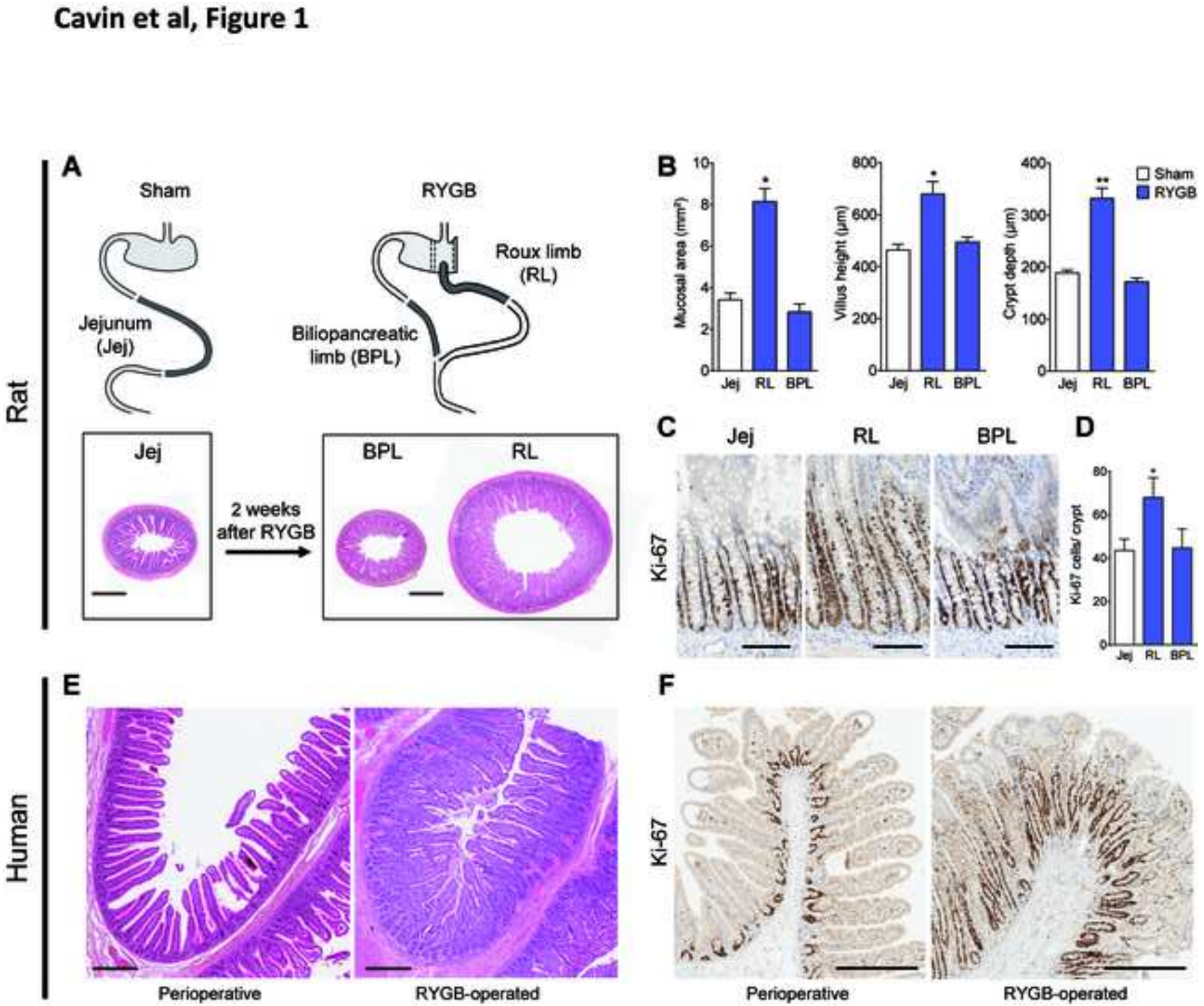


Figure 2
Click here to download Figure: Cavin et al Figure 2.tif

Cavin et al, Figure 2

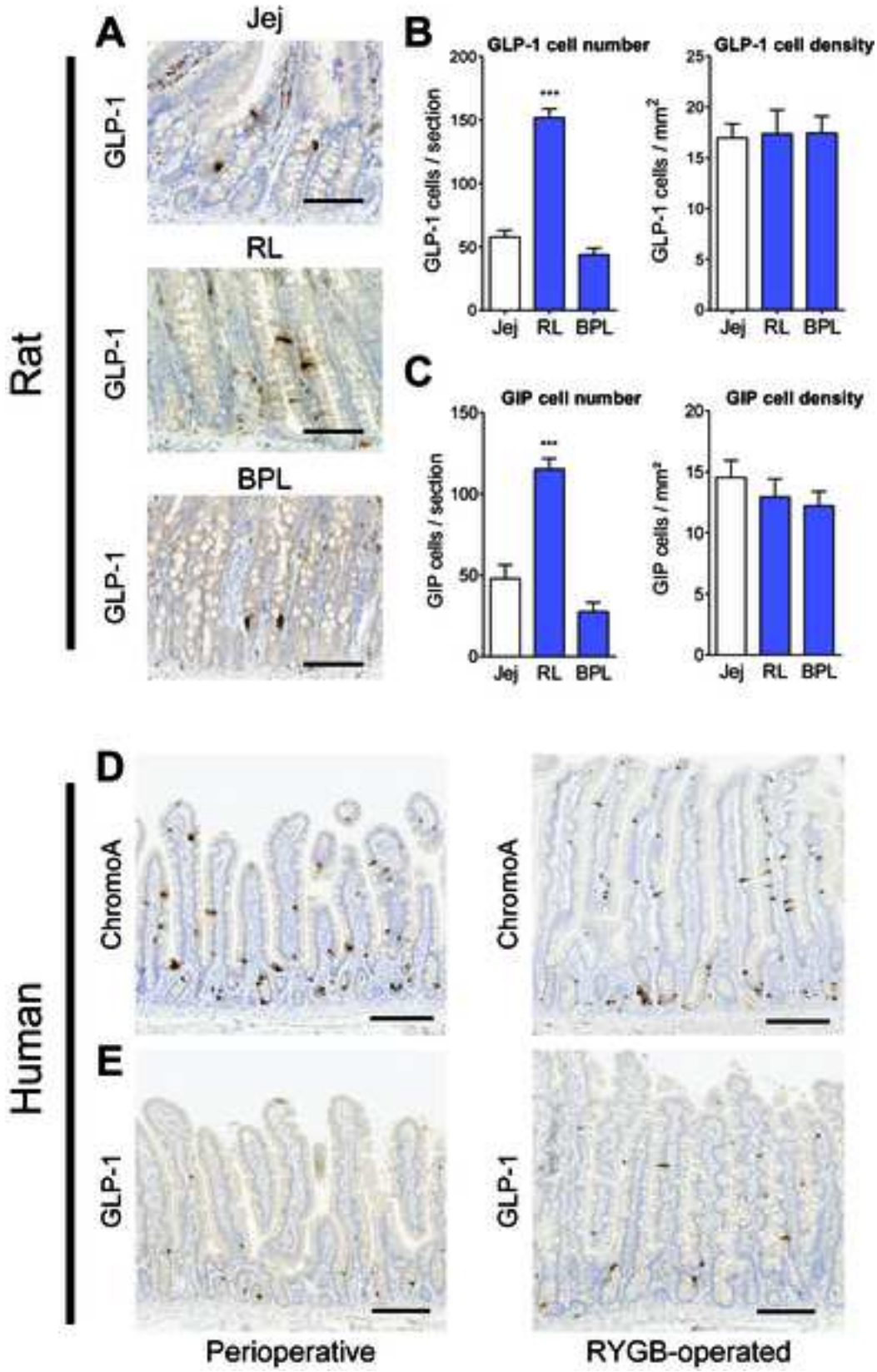


Figure 3
Click here to download Figure: Cavin et al Figure 3.tif

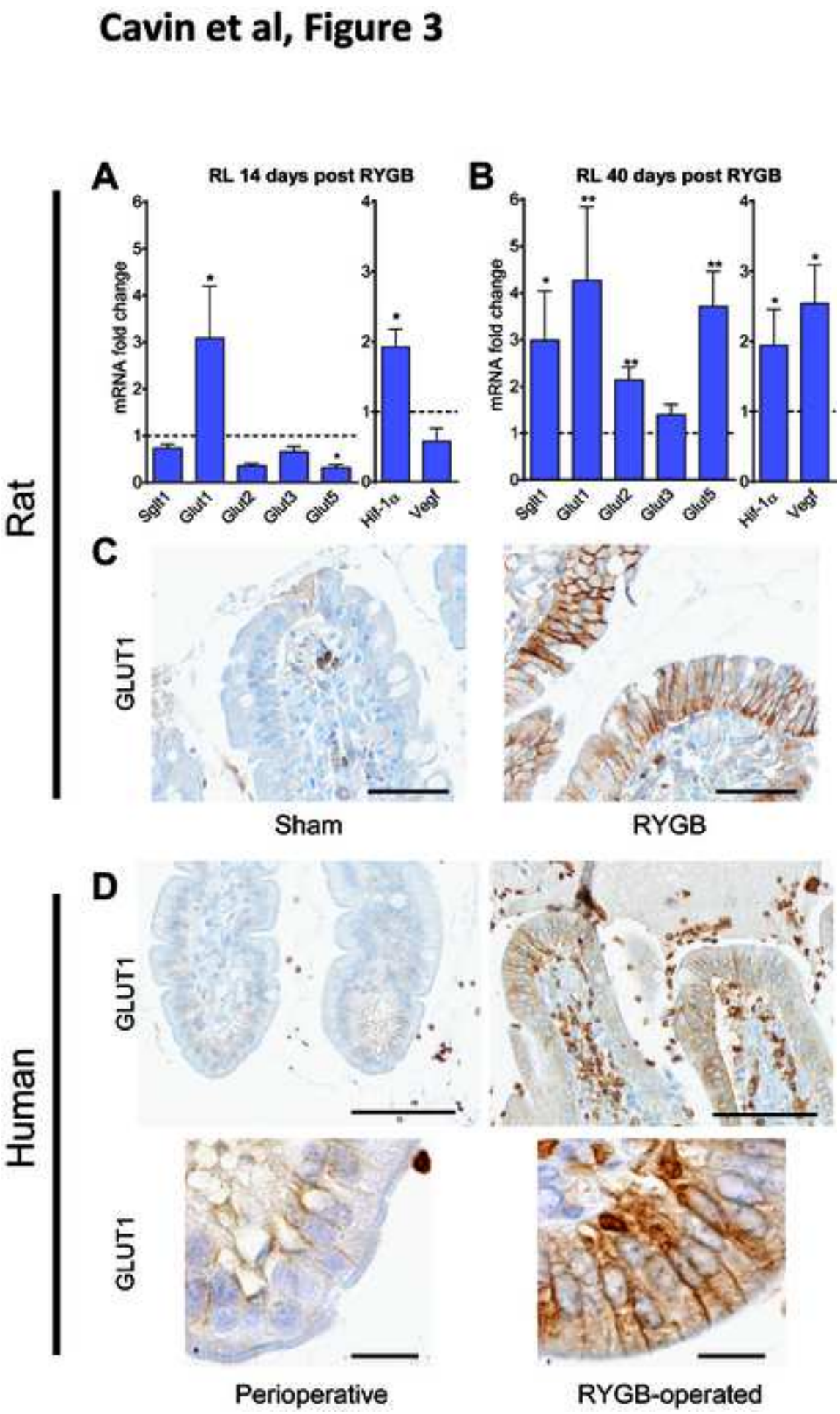


Figure 4

Click here to download Figure: Cavin et al Figure 4.tif

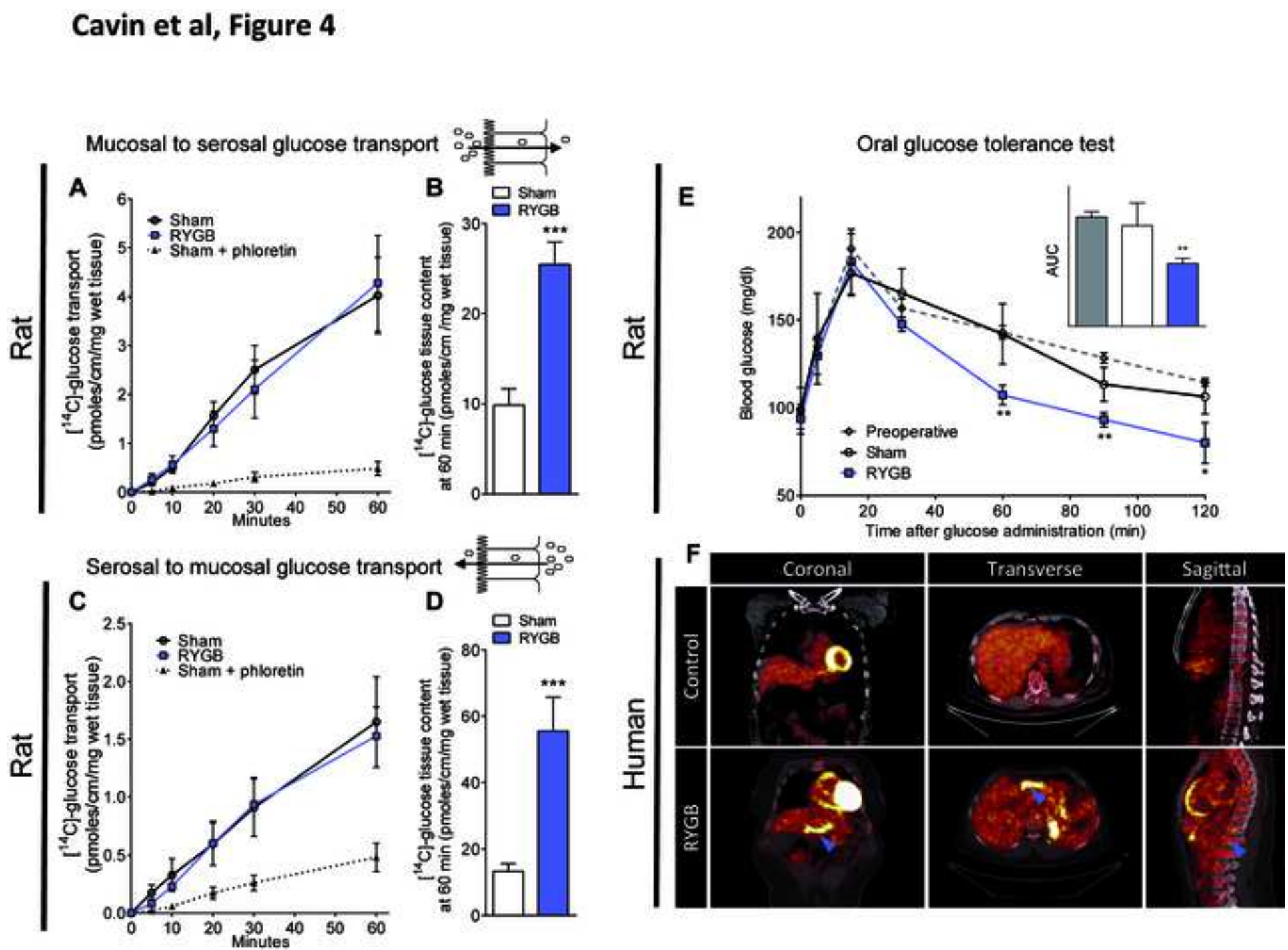


Figure 5

Click here to download Figure: Cavin et al Figure 5.tif

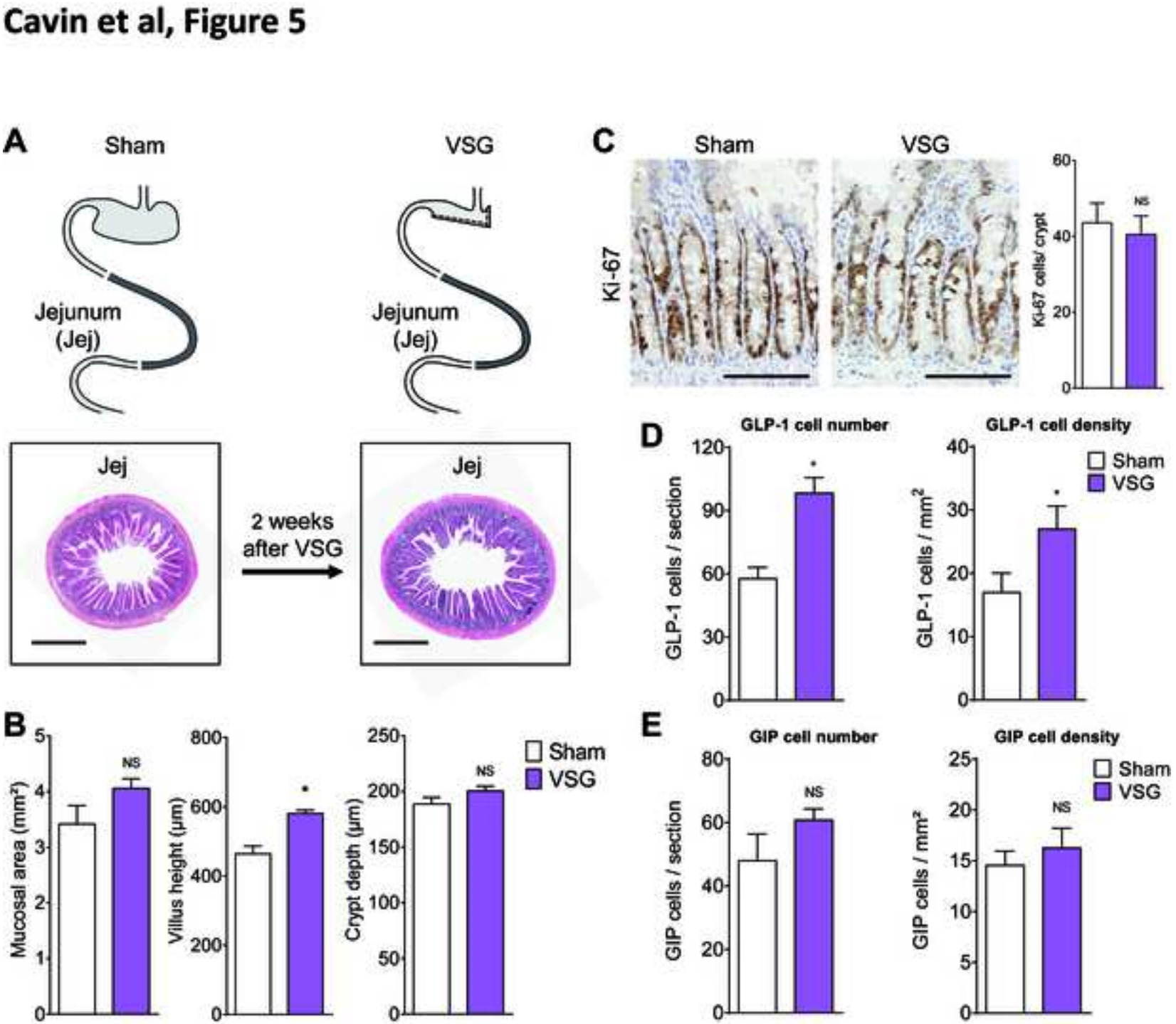


Figure 6

Click here to download Figure: Cavin et al Figure 6.tif

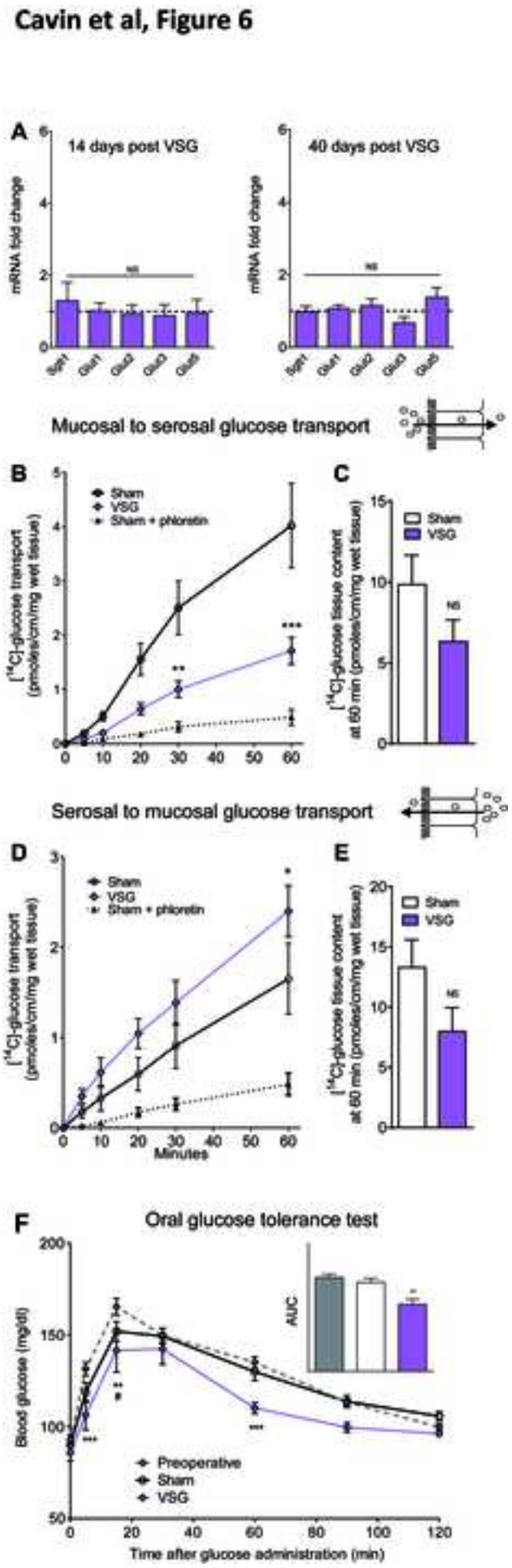
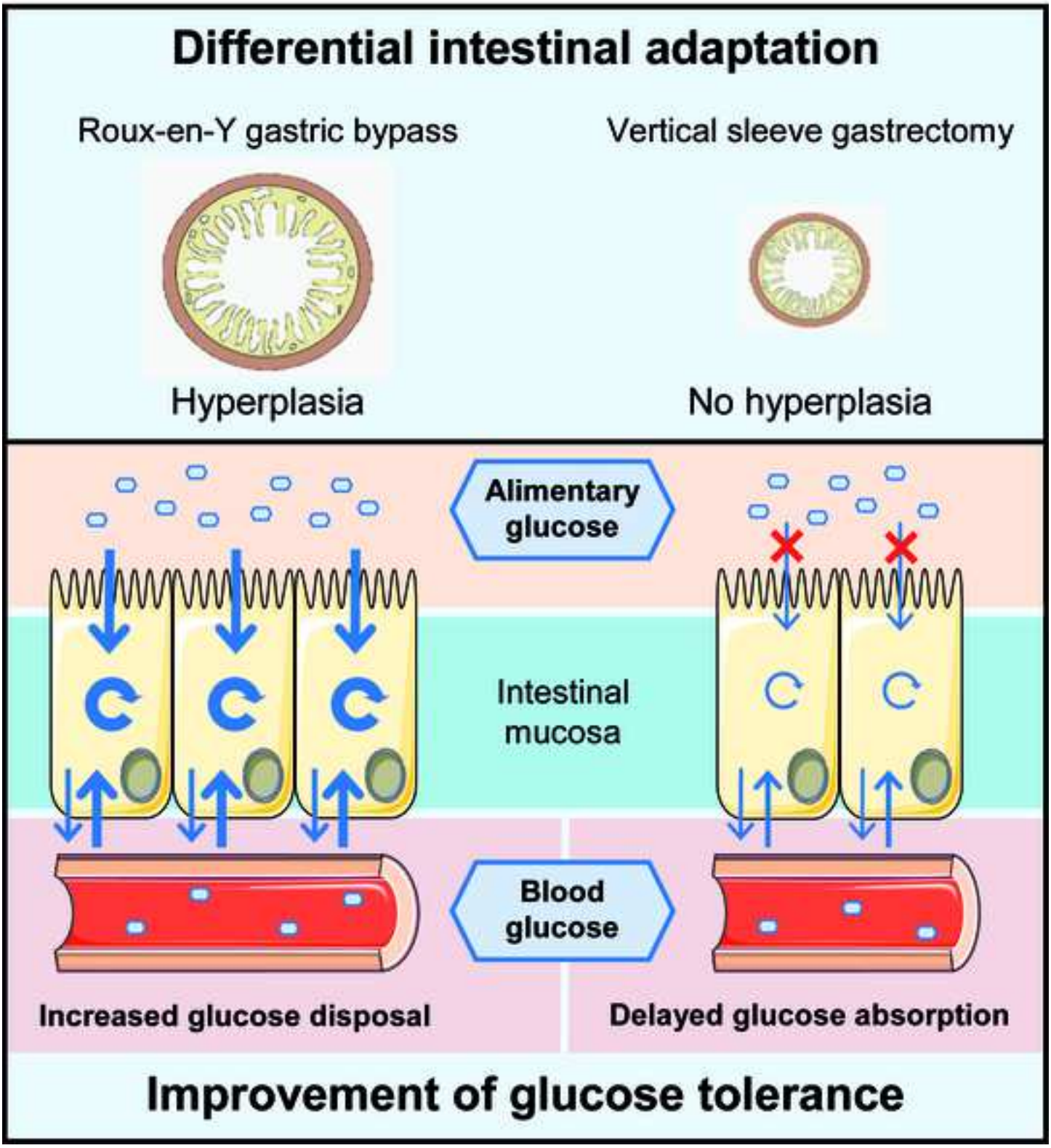


Figure 7
Click here to download Figure: Cavin et al Figure 7.tif

Cavin et al, Figure 7



Supporting Document NO Tracked Changes
Click here to download Supporting Document: Revised Supporting documents NO Tracked Changes.doc

SUPPORTING DOCUMENTS

Supplemental Experimental Procedures

Animal surgeries and post-surgery procedures

Male Wistar rats weighing 220–240 g were fed with high-fat diet (HFD, Altromin C45) for 16 weeks. Diet-induced obese rats weighing 675 ± 50g were divided into Roux-en-Y gastric bypass (RYGB), sleeve gastrectomy (VSG) and sham-operated (sham) group. They were fasted overnight before operation. Anesthesia was induced by intraperitoneal injection of pentobarbital (Ceva, Libourne, France). Standard aseptic procedures were used throughout. After laparotomy, the stomach was isolated outside the abdominal cavity. Loose gastric connections to the spleen and liver were released along the greater curvature, and the suspensory ligament supporting the upper fundus was severed.

RYGB: The forestomach was resected using an Echelon 45-mm staple gun with blue cartridge (Ethicon, Issy les Moulineaux, France). Then, the gastric pouch was created with a TA-DST 30-mm-3.5-mm stapler (Covidien, Courbevoie, France) preserving the arterial and venous supply. The jejunum was transected 15 cm distally from the pylorus. The Roux limb was anastomosed to the gastric pouch and the biliopancreatic limb was anastomosed 20 cm distally to gastro-jejunal anastomosis with 6-0 Polydioxanone (PDS) running sutures.

VSG: After resection of the forestomach as above, 80% of the stomach was resected with an application of Echelon 45-mm staple gun, leaving a thin gastric tube in continuity with the esophagus and keeping the antrum in place.

Sham: To mimic surgery, stomach was tweaked with an unarmed staple gun for RYGB sham and VSG sham and jejunum was transected and repair for RYGB sham.

For all these procedures, the laparotomy was closed with 5.0 Polyglycolide (PGA) suture in two layers.

Post-operative care:

Health and behavior of each animal were evaluated daily.

RYGB-operated rats were kept without food for 48 h after the surgery. They received subcutaneous injections of 12 mL Bionolyte G5 (Baxter, Maurepas, France) twice a day within this period. From days 3 to 5, they had access to liquid diet (Altromin C-0200, Genestil, Royaucourt, France), which correspond to 50 Kcal/day (50% of preoperative intake). A free access to solid Normal Diet (Altromin 1324, Genestil, Royaucourt, France), was allowed from day 6.

VSG-operated rats were kept without food for 24 h after the surgery but they received subcutaneous injections of 12 mL Bionolyte G5 (Baxter, Maurepas, France) twice a day. From days 2 to 3, they had access to liquid diet (Altromin C-0200, Genestil, Royaucourt, France), which correspond to 50 Kcal/day (50% of preoperative intake). A free access to solid Normal Diet (Altromin 1324, Genestil, Royaucourt, France), was allowed from day 4. Sham-operated rats had the same post-operative care than their corresponding surgical group.

Post-operative analyses: Body weight and food intake were measured daily and the average daily calorie intake was calculated. Fourteen or forty days after surgery, rats were euthanized after overnight food deprivation and gut segments were sampled as illustrated (Figure S1).

Stool analyses

10 days after surgery, rats were transferred into metabolism cages. The total amount of consuming food was recorded each day. The stools were collected daily and stored at -20°C. Stools collected for three days were pooled, and analyses were performed on homogenized samples. Total energy content was determined by bomb calorimetry (PARR 1351 Bomb Calorimeter; Parr Instrument Company). Fecal calorie loss represented the proportion of ingested energy recovered in stool output.

Oral glucose tolerance test

Rats were fasted for 16 h before being subjected to an oral glucose tolerance test (OGTT). Blood was sampled from the tail vein before (t=0) and 5, 15, 30, 60, 90 and 120 min after oral load of glucose (1g/kg body weight). Blood glucose levels were measured with the AccuChek System (Roche Diagnostics, Meylan, France) and expressed in mg/dL.

Plasma GLP1 measurement

Rats were fasted for 16 h before being subjected to an oral load of glucose (1g/kg body weight). Blood (200μL), sampled from the tail vein before (t=0) and 30 after the gavage, was collected in presence of DPPIV inhibitor (Roche) to limit degradation of active GLP1. Rat plasma concentrations of active GLP1 was quantified on a Luminex MagPix200 analyzer using Milliplex rat gut hormone panel (RMHMAG-84K Merck Millipore).

Histology and Immunohistochemistry

As a routine process, when obese patients undergo RYGB surgery, a sample is taken from the jejunum in close contact to the anastomosis. When patients are operated on for complication after RYGB, the gastro-jejunal anastomosis is resected and a sample of jejunum is taken 5 cm far from the anastomosis for analyses. RYGB patients were undergoing re-operations for persistent ulcers, dumping syndrome or pouch dilations one to five years after the initial RYGB surgery (Please see TableS 1 for detailed description of the patients). In rats, gut segments were sampled as illustrated (Figure S1) fourteen days or forty days after surgery.

Rat and human samples were immediately fixed overnight in formalin. Three µm blank slides were cut from each block to perform either hematoxylin phloxine saffron (HPS) staining or immunostaining with Ki67, GLP1, Chromogranin A, GIP and GLUT1 antibodies.

Immunohistochemistry was carried out using an automated immunohistochemical stainer according to the manufacturer's guidelines (Bond-Max autostainer, Leica, Wetzlar, Germany), after dewaxing and rehydrating paraffin sections and antigen retrieval by pretreatment with high temperature at pH 9. After antigen retrieval, tissue sections were immunolabelled with primaries antibodies used as follows: Rat Ki67 (Dako M7248): diluted 1:25, pH6; Human Ki67 (Dako M7240): diluted 1:100, pH9; Rat GLUT1 (spring bioscience E2844): diluted 1:200, pH6; Human GLUT1 (AnaSpec 53519): diluted at 1:200, pH6; Human Chromogranin A (DAKO M0869): diluted 1:250, pH6; Rat GIP (Peninsula Laboratories T-4053): diluted 1:3000, pH6; Rat GLP1 (Abcam AB26278): diluted 1:3000, pH9. Substitution of the primary antibody with PBS was used as a negative control. Subsequently, tissues were incubated with secondary antibody polymer for 10 min (Bond Polymer Refine detection; DS9800; Leica Microsystems) and developed with DAB-Chromogen for 10 min. Internal positive controls consisted in red blood cells for GLUT1 and nucleus of crypt cells for Ki67. Immunostainings were evaluated by two pathologists blinded to the clinical data AC and MH from the department of Pathology of Bichat Hospital. Each slide was scanned with an Aperio ScanScope® CS System (Leica Microsystemes SAS, Nanterre France). Morphometric analyses were performed using the Calopix Software (TRIBVN, Chatillon, France) on three to four distant sections per rat sample. The number of Ki67 immunoreactive cells per crypt was evaluated in 3-4 crypts from three to four cross sections from each intestinal limb for each animal. Averages were used for statistical analyses.

Reverse transcription and Quantitative Real-time PCR

Total RNA was extracted from frozen intestinal mucosa scrapings with TRIzol reagent (Invitrogen, Saint Aubin, France). One µg from each sample was converted to cDNA using the Verso cDNA Synthesis Kit (Thermo Scientific, Waltham, MA, USA). Primers were designed using Roche assay design center or were based on previous studies; they were all synthesized by Eurogentec (Angers, France). Real-time PCR was perfomed using the Light

Cycler 480 system (Roche Diagnostics, Indianapolis, IN, USA) according to the manufacturer's instructions under the following conditions: 15 min denaturation at 95°C, followed by 50 cycles of 10 sec at 95°C, 45 sec at 60°C and 10 sec at 72°C. Melting curves were performed for each reaction, from 55°C to 95°C at 0.11°C/sec. Ct values of the gene of interest were normalized with two different reference genes (L19 and HPRT) which were chosen after multiple comparisons with numerous reference genes. The primers used in this study are presented below.

Gene	**NCBI Accession #**	**Sequence**
Glut1	NM_138827	GTGCTCGGATCCCTGCAGTTCG
		GGGATGGACTCTCCATAGCGGTG
Glut2	NM_012879	AAAGCCCCAGATACCTTTACCT
		TGCCCCTTAGTCTTTTCAAGC
Glut3	NM_017102	GCGCAGCCCTTCCGTTTTGC
		CGCTGGAGGATCTCCGTCGC
Glut5	NM_031741	GCCTTCGGAGTGTCTTGG
		GGCAGGGACTCCAGTCAG
Hif1α	NM_024359	AAGCACTAGACAAAGCTCACCTG
		TTGACCATATCGCTGTCCAC
Hprt	NM_012583	GACCGGTTCTGTCATGTCG

		ACCTGGTTCATCATCACTAATCAC
L19	NM_031103	TGCCGGAAGAACACCTTG
		GCAGGATCCTCATCCTTCG
Sglt1	NM_013033	GAAGGGTGCATCGGAGAAG
		CAATCAGCACGAGGATGAAC
Vegf	NM_031836	GAGTTAAACGAACGTACTTGCAGA
		TCTAGTTCCCGAAACCCTGA

SGLT1 activity measurement

Intestine segments were opened along the mesenteric border and placed between the two halves of an Ussing chamber (Easy Mount P2312; Physiologic Instrument, San Diego, CA, USA) (exposed area: 0.50 cm2). Tissues were bathed with 4 ml of KRB solution with glucose 10 mM in serosal compartment and mannitol 10 mM in mucosal compartment. Solutions were gassed with 95% O2–5% CO2 and kept at a constant temperature of 37°C. Electrogenic ion transport was monitored continuously as the short-circuit current (Isc) by an automated voltage clamp apparatus (DVC 1000; WPI, Aston, England, UK) linked through a Lab-Trax-4 interface to a computer. Tissue ionic conductance was calculated according to Ohm's law. Sodium-dependent glucose transporter SGLT1 was challenged by 10 mM glucose. Results were expressed as the difference (ΔIsc) between the peak Isc (measured within 10 min) and the basal Isc (measured just before the addition of glucose).

Glucose transport and consumption assay

Glucose transport was assayed ex vivo using jejunal loop as described previously [1]. Briefly, four 3-cm intestinal segments were filled with Krebs Ringer Bicarbonate Buffer solution containing 30 mM D-glucose with 0.1 µCi/ml [14C]-glucose (specific activity 49.5 mCi/mmoL) and with or without 100 µM phloretin, a glucose transporter inhibitor. Each segment were ligated at both ends and incubated in a 37°C thermostat-controlled bath of Krebs modified buffer at pH 7.4 continuously gassed with 95% O2-5% CO2. Mucosal-to-serosal and serosal-to-mucosal transport of glucose, were monitored using everted and non-everted isolated intestinal loops, respectively. Time dependent [14C]-glucose transport was determined by sampling from the bath at 0, 5, 10, 20, 30 and 60 min. At 60 min, isolated intestinal loops were collected, flushed, weighed, and homogenized with ultraturax for quantification of radioactivity. Radioactivity was measured using a beta counter (Beckman LS 6000 TA liquid scintillation counter). Apparent permeability (Papp) was used to assess transport according to the following equation $Papp=(dQ/dt)\cdot(V/Q0\cdot A)$, where V is the volume of the incubation medium, A is the area of the loop, Q0 is the total radiolabeled glucose introduced into the loop and dQ/dt is the flux across the intestinal loop.

Positron emission tomography

Seven patients were retrospectively selected from the files of the department of nuclear medicine, Bichat Hospital, France. Three RYGB patients and four control patients (without gastro-intestinal diseases or cancer) had been evaluated with [18F]-FDG PET/CT for the detection of workup of thoracic tumours, Horton disease or detection of site of infection or inflammation. The patients were imaged on average 4 years after surgery (Please see Table S2 for detailed description of the patients). PET and CT were performed with a PET/CT hybrid system (Discovery 690; GE Healthcare). Imaging started 60 min after 18F-FDG injection with a non-enhanced, low-dose CT scan (120 kV, 80 mA), which was followed by a whole-body PET acquisition in 3-dimensional mode with an acquisition time of 4 min per bed

position. PET Imaging was performed only if the fasting glucose level was lower than 7.7 mmol/L before [18F]-FDG injection. Mean glycaemia was 4.9 ± 0.4 mmol/L in the RYGB group and 5.9 ± 1.1 mmol/L in the control group. [18F]-FDG was injected intravenously at a dose of 4 MBq/kg; mean dose was 295 ± 66 MBq in the RYGB group and 361 ± 110 MBq in the control group. [18F]-FDG PET acquisitions were interpreted using the Advantage Workstation of the PET/CT system (GE Healthcare) by two experienced nuclear medicine physicians, who were blinded to the subject's group status. Both physicians worked separately; then, in case of discrepancies, they reviewed the images together in order to reach a consensus. Image analysis was based on visual interpretation and semi-quantitative measurement of [18F]-FDG uptake. On visual analysis, abnormal hypermetabolic activity in the abdominal areas was classified as positive or negative and increased [18F]-FDG uptake in this area was confirmed on non–attenuation-corrected PET images.

Statistical analyses

Statistical analyses were performed with GraphPad Prism version 6.0 (GraphPad Software, SanDiego, CA, USA). Areas under the curves (AUC) were calculated using the trapezoid rule.

Table S1. Patients included for histologic analyses

		Sexe	Age	BMI	Indication for reoperation	Time after RYGB surgery (month)
RYGB operated group*	Patient 1	F	30	37	Persistent ulcer	12
	Patient 2	M	32	36	Dumping syndrome	29
	Patient 3	F	46	38,8	Weight regain and pouch dilation	36
	Patient 4	F	50	39,9	Persistent ulcer	53
	Patient 5	F	56	27,8	Persistent ulcer	60
Obese control group	Patient 1	F	65	54,2	NA	NA
	Patient 2	M	38	49,8	NA	NA
	Patient 3	M	58	61	NA	NA

*None of those patients have experienced intestinal obstruction or any other known issues which could have directly impacted the histologic characteristics of the samples.

Table S2. Patients included for [18F]-FDG PET/CT scan analyses

		Sexe	Age	BMI	Time after RYGB surgery (month)
RYGB operated group	Patient 1	F	54	27,7	48
	Patient 2	F	49	27,8	38
	Patient 3	F	64	33,3	50
Control group	Patient 1	M	73	28,8	NA
	Patient 2	F	80	29,1	NA
	Patient 3	F	56	36,7	NA
	Patient 4	M	49	27,7	NA

Text S1.

To evaluate the histologic and functional adaptation of the alimentary Roux limb after surgery, we performed RYGB in diet-induced obese rats (Figure S2A and S2B). Male Wistar rats fed a high-fat diet for 4 months, were operated and subjected to post-operative care for 6 days before having access ad libitum to solid normal diet. The combination of surgical procedure and postoperative care with liquid diet (caloric restriction) led to a substantial weight loss which was higher in RYGB compared to sham-operated rats (Figure S2C). Weight loss was primarily due to a decrease in food intake (Figure S2D) rather than malabsorption, since fecal calorie loss did not change significantly after surgery (Figure S2E). The incidental role played by malabsorption, compared to decrease in food intake, on weight loss has already been described in few studies[2,3] . RYGB-operated rats displayed an improved oral glucose tolerance compared to preoperative state at 12 days post-surgery (Figure 4). Caloric restriction during intensive post-operative care period, weight loss and diet switch were not sufficient to trigger improvement of glucose tolerance in sham-operated rats compared to preoperative state (Figure 4). This data highlights the crucial role of surgery on initial post-operative glycemic improvement.

Text S2.

To directly compare the histologic and functional adaptation of the jejunum after VSG and RYGB, we performed VSG in diet-induced obese rats (Figure S6). Operated VSG and Sham rats were subjected to post-operative care for 3 days before having access ad libitum to solid normal diet. The combination of surgical procedure and postoperative care with liquid diet (caloric restriction) led to a substantial weight loss which was higher in VSG compared to sham-operated rats (Figure S6A). Weight loss was primarily due to a decrease in food intake (Figure S6B). Caloric restriction during intensive post-operative care period, weight loss and diet switch were not sufficient to trigger improvement of glucose tolerance in sham-operated rats at 12 days post-surgery compared to preoperative state (Figure 6F). On the contrary,

VSG-operated rats displayed an improved oral glucose tolerance compared to preoperative state at 12 days post-surgery (Figure 6F). This data highlights the crucial role of surgery on initial post-operative glycemic improvement. Of note, the difference in weight loss and food intake in VSG-Sham and RYGB-Sham rats is due to difference in post-operative care. VSG-Sham rats had access to normal food as soon as 4 days post-surgery and lost less weight than sham RYGB-Sham rats who had access to normal food ad libitum only after 6 days post-surgery (Figure S2C and S6A). However, jejunal adaptation and intestinal glucose handling 2 weeks post-surgery were not different between RYGB-Sham and VSG-Sham confirming that weight loss and caloric restriction *per se* were not responsible for intestinal adaptation and improved glucose tolerance observed after RYGB or VSG.

Figure S1. Sampling of intestinal segments

Figure S2.

(A) Postmortem macroscopic views of rat stomach 14 days after sham (upper panel) or RYGB surgery (lower panel). The RYGB procedure results in ingested food flowing from the esophagus (oe) to the gastric pouch (g.po) and then directly to the jejunum (jej) of the Roux limb, bypassing the distal stomach (d.st), the duodenum (du), and part of the proximal jejunum.

(B) Postmortem view of the gastrointestinal tract of a rat after RYGB surgery, showing the lengths of the Roux limb, biliopancreatic limb (which drains gastric, hepatobiliary and pancreatic secretions), and common limb after RYGB with, in continuity, the cecum and the colon. The red dotted line indicates the new path followed by food.

(C) Loss of body weight after surgery in RYGB- (n = 11) and sham-operated rats (n = 9). The black box corresponds to the period of postoperative care (5 days) before the animals had free access to solid normal diet. The data shown are means ± SEM.

(D) Changes in daily calorie intake after surgery. The dotted line indicates mean calorie intake before surgery. The data shown are means ± SEM. **P < 0.01, ***P < 0.001, versus preoperative value, in Mann-Whitney tests.

(E) Loss of fecal calories, determined by bomb calorimetry analyses of stools collected on day 12 after surgery. Results are expressed as a percentage of calorie intake.

Figure S3.

(A) Morphometric analyses showing the mucosal area of RL and BPL sections of rats subjected to RYGB surgery (n = 5), compared with the corresponding jejunum segment from sham-operated rats (Jej) (n = 5) 40 days after surgery. Data are means ± SEM. **P < 0.01 versus sham-operated rats, based on ANOVA with Bonferroni correction for multiple comparisons.

(B) Morphometric analyses showing the mucosal area of sections from VSG-rats (n = 5), compared with the corresponding jejunum segment from sham-operated rats (n = 5) 40 days after surgery. Data are means ± SEM. NS, not significant, in Mann-Whitney tests.

Figure S4.

Plasma active GLP1 levels in fasted rats (A) or 30min after an oral load of glucose (1g/kg) (B) 12 days after RYGB (n = 5) VSG (n = 4) or sham surgery (n = 3). Data are means ± SEM. *P < 0.05 (vs. sham), in two-way ANOVA with Bonferroni correction for multiple comparisons.

Figure S5.

(A and B) Relative mRNA levels of sugar transporters and hypoxia inducible genes in the biliopancreatic limb mucosa (A) 14 days (n = 4) and (B) 40 days (n = 6) after RYGB. The dotted line indicates the mean mRNA level of the corresponding genes in jejunal mucosa from sham-operated rats (n = 5). Data are means ± SEM. *P < 0.05, versus sham-operated rats, in Mann-Whitney tests.

Figure S6.

(A) Loss of body weight after surgery in VSG- (n = 9) and sham-operated rats (n = 7). The black box corresponds to the period of intensive postoperative care (3 days) before the animals had free access to solid normal diet. The data shown are means ± SEM.
(B) Changes in daily calorie intake after surgery. The dotted line indicates mean calorie intake before surgery. The data shown are means ± SEM. ***P < 0.001, versus preoperative value, in Mann-Whitney tests.

Supplemental References

1. Tavernier A, Cavin J-B, Gall ML, et al. Intestinal deletion of leptin signaling alters activity of nutrient transporters and delayed the onset of obesity in mice. FASEB J. 2014;28:4100–4110.
2. Odstrcil EA, Martinez JG, Ana CAS, et al. The contribution of malabsorption to the reduction in net energy absorption after long-limb Roux-en-Y gastric bypass. Am. J. Clin. Nutr. 2010;92:704–713.
3. Sandoval D. Bariatric surgeries: beyond restriction and malabsorption. Int. J. Obes. 2011;35:S45–S49.

Figure S1
Click here to download Figure: Cavin et al Figure S1.tif

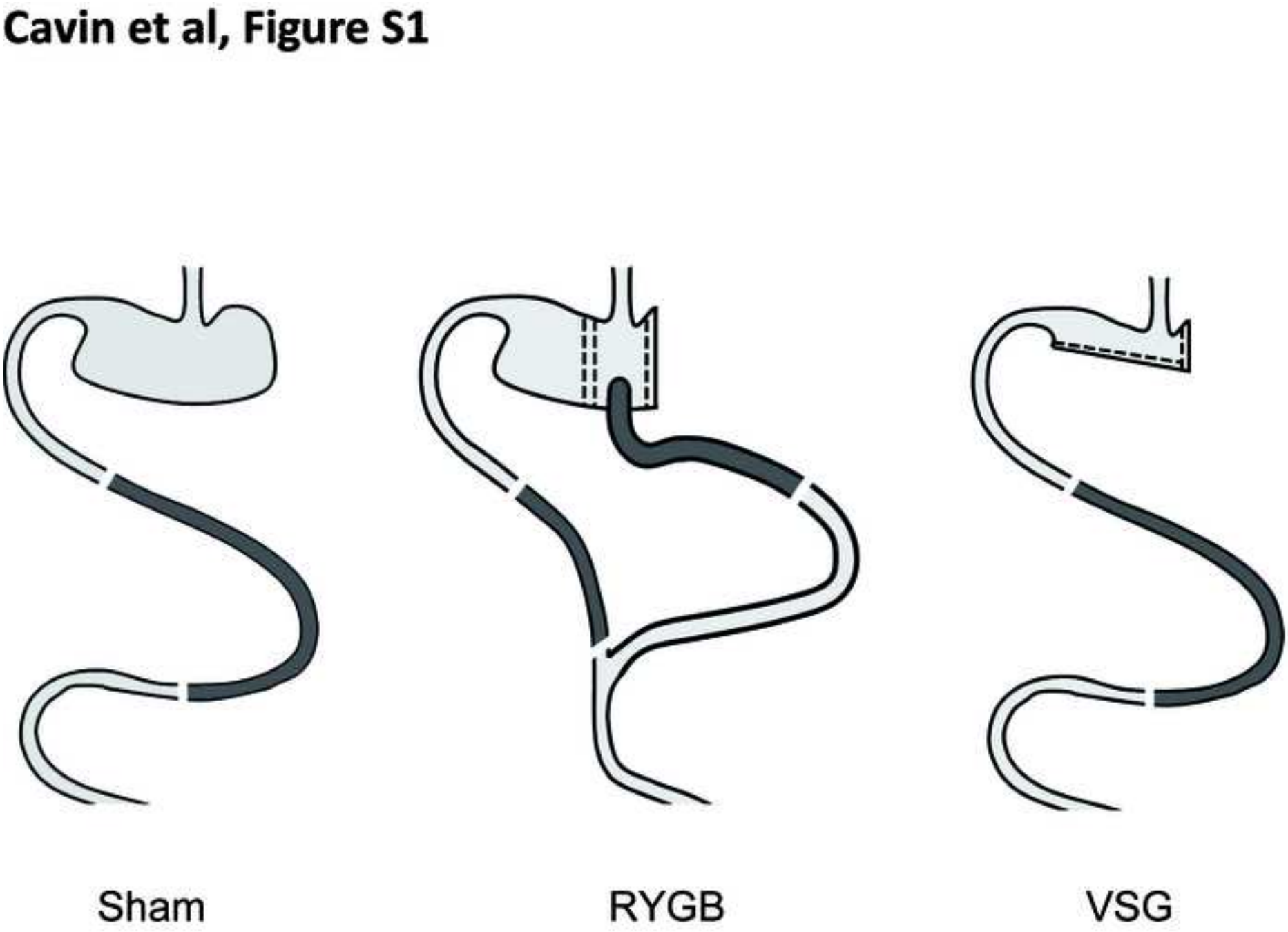


Figure S2
Click here to download Figure: Cavin et al Figure S2.tif

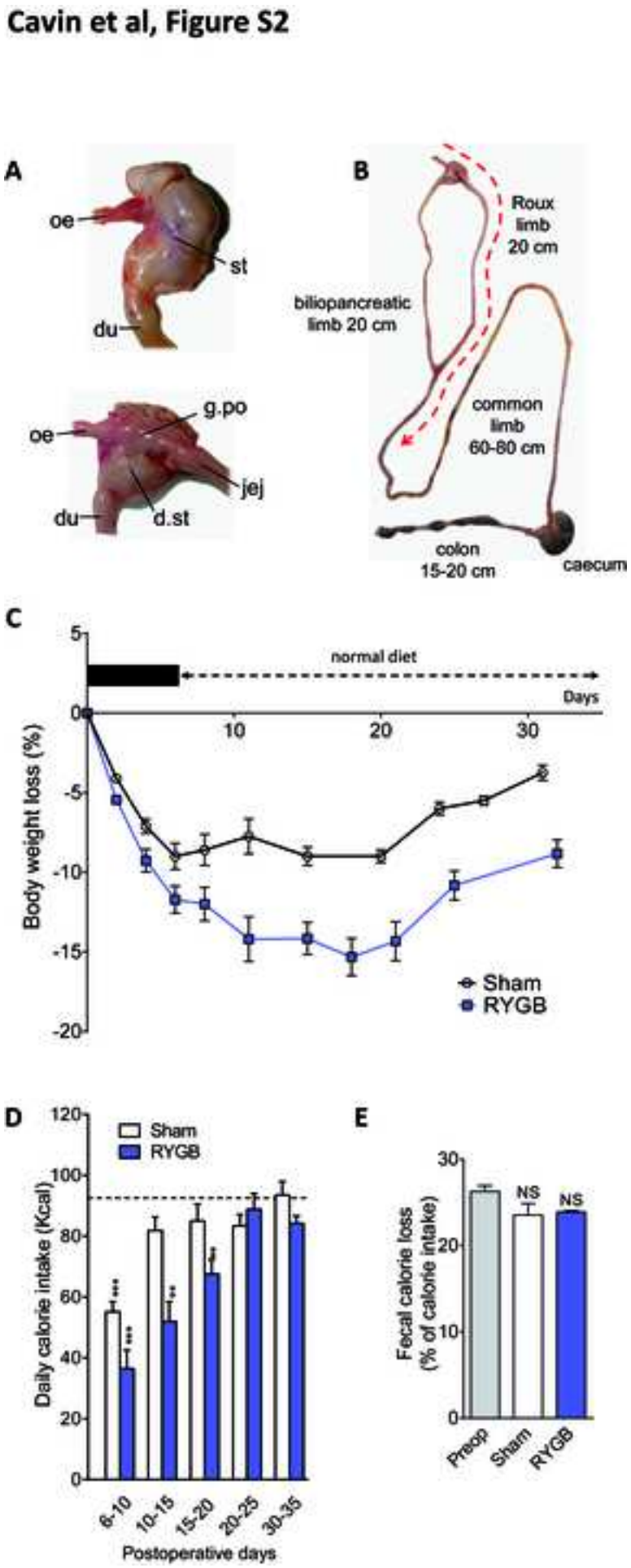


Figure S3
Click here to download Figure: Cavin et al Figure S3.tif

Cavin et al, Figure S3

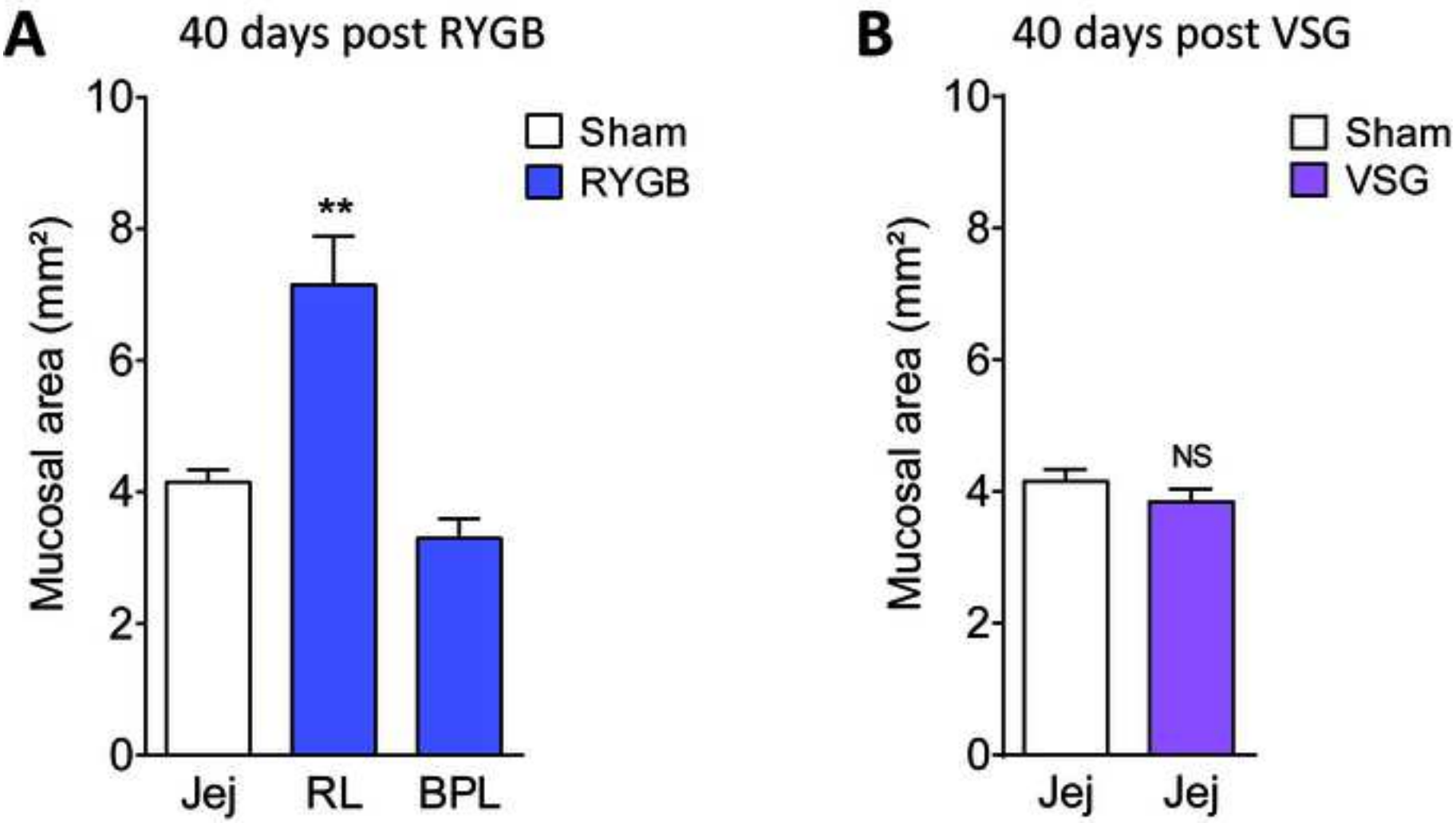


Figure S4
Click here to download Figure: Cavin et al Figure S4.tif

Cavin et al, Figure S4

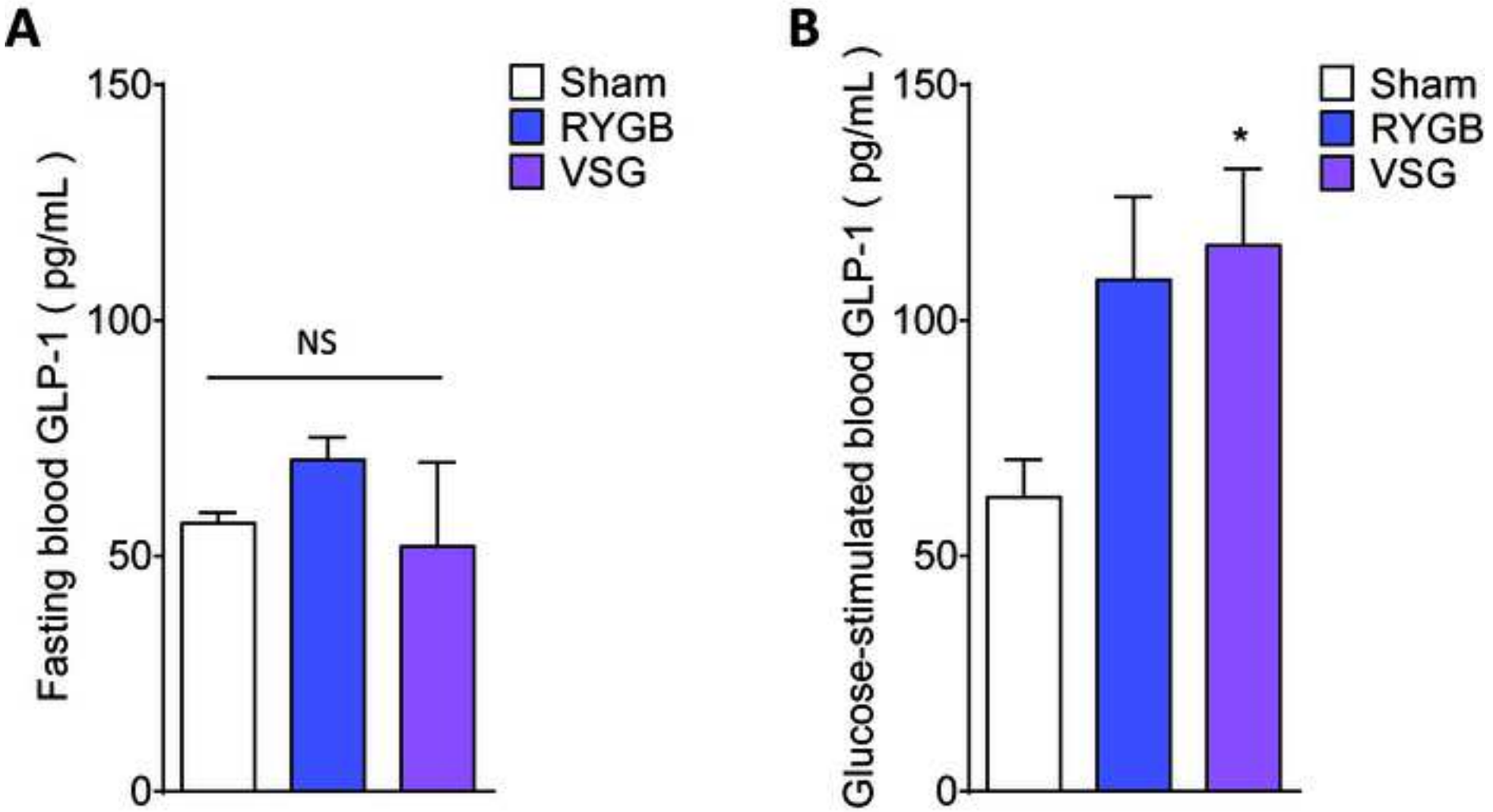


Figure S5
Click here to download Figure: Cavin et al Figure S5.tif

Cavin et al, Figure S5

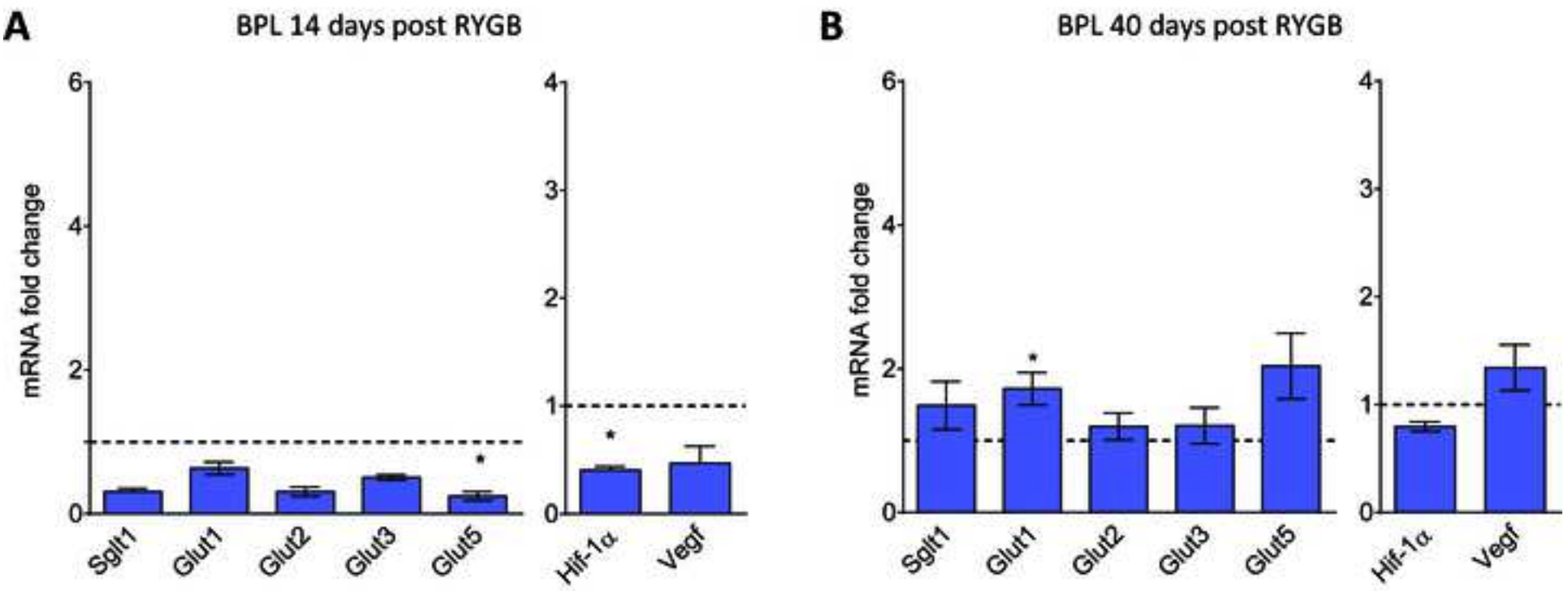
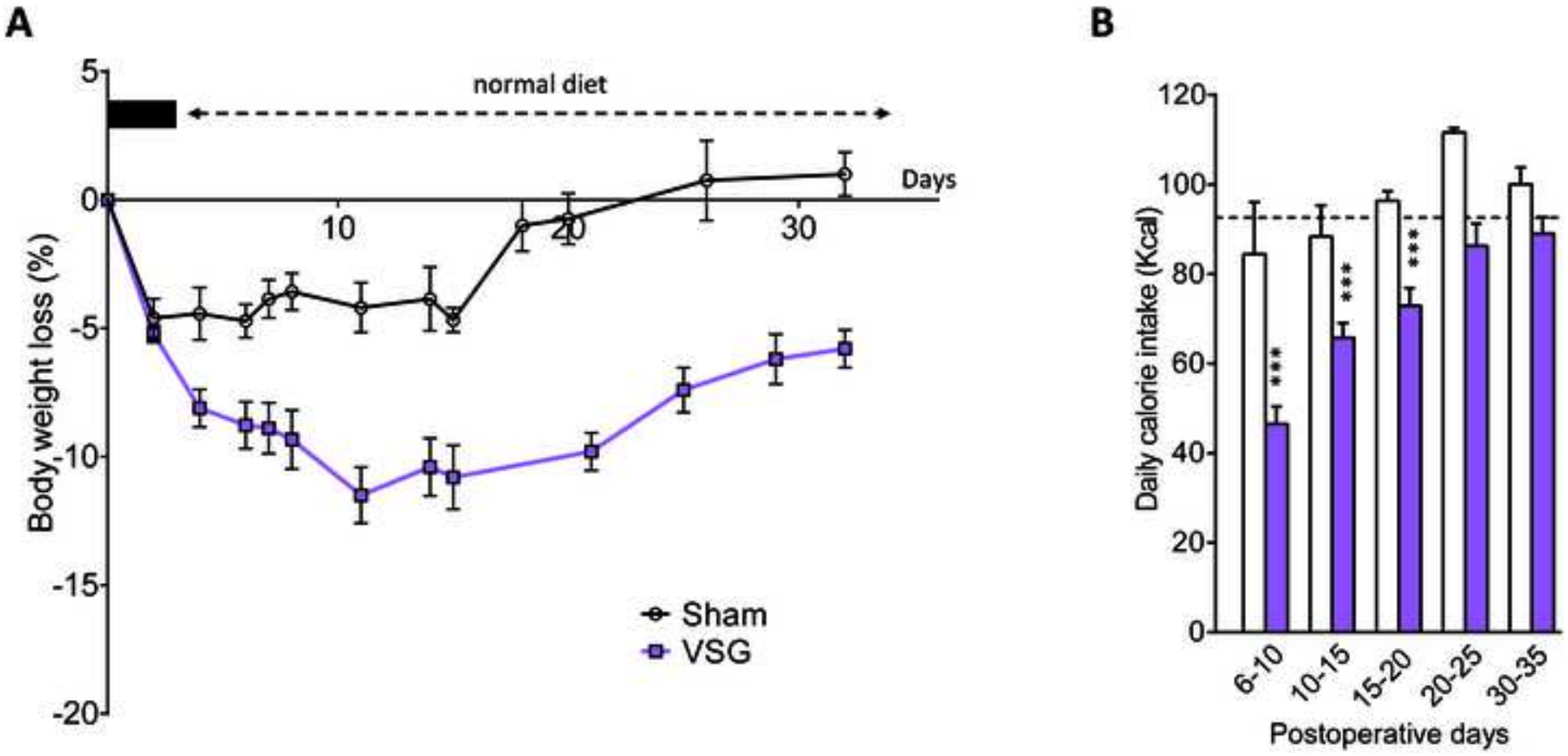


Figure S6
Click here to download Figure: Cavin et al Figure S6.tif

Cavin et al, Figure S6



Movie S1

Click here to download Video (supplemental): Movie S1.mp4

Revised Manuscript in Word or RTF (no changes marked)
Click here to download Revised Manuscript in Word or RTF (no changes marked): Revised Manuscript Cavin et al. NO tracked changes.d